Coverage Analysis of a Vehicular Network Modeled as Cox Process Driven by Poisson Line Process

Vishnu Vardhan Chetlur and Harpreet S. Dhillon

***Abstract*—In this paper, we consider a vehicular network in which the wireless nodes are located on a system of roads. We model the roadways, which are predominantly straight and randomly oriented, by a Poisson line process (PLP) and the locations of nodes on each road as a homogeneous 1D Poisson point process (PPP). Assuming that each node transmits independently, the locations of transmitting and receiving nodes are given by two Cox processes driven by the same PLP. For this setup, we derive the coverage probability of a typical receiver, which is an arbitrarily chosen receiving node, assuming independent Nakagami-m fading over all wireless channels. Assuming that the typical receiver connects to its closest transmitting node in the network, we first derive the distribution of the distance between the typical receiver and the serving node to characterize the desired signal power. We then characterize coverage probability for this setup, which involves two key technical challenges. First, we need to handle several cases as the serving node can possibly be located on any line in the network and the corresponding interference experienced at the typical receiver is different in each case. Second, conditioning on the serving node imposes constraints on the spatial configuration of lines, which requires careful analysis of the conditional distribution of the lines. We address these challenges in order to characterize the interference experienced at the typical receiver. We then derive an exact expression for coverage probability in terms of the derivative of Laplace transform of interference power distribution. We analyze the trends in coverage probability as a function of the network parameters: line density and node density. We also provide some theoretical insights by studying the asymptotic characteristics of coverage probability.**

***Index Terms*—Stochastic geometry, Cox process, Poisson line process, coverage probability, vehicular network, road systems, Nakagami-m fading.**

I. Introduction

Vehicular communication, which collectively refers to vehicle-to-vehicle (V2V) and vehicle-to-infrastructure (V2I) communication, has enabled the vehicular nodes to share information with each other and also with roadside units (RSUs) to improve the road safety and transport efficiency [2]–[4]. With autonomous vehicles becoming a reality in the near future, the data traffic originating from vehicular networks is expected to increase many folds while also putting more stringent latency and connectivity constraints compared to the networks of today. In order to meet these stringent requirements, it is critical to understand the system-level performance of these networks under different operational scenarios. In the recent years, stochastic geometry has emerged as a powerful tool for modeling and system-level analysis of wireless networks. The most popular approach is to model the locations of wireless nodes by a homogeneous 2D Poisson point process (PPP) [5]–[8] and focus on the performance analysis of a randomly chosen receiver in the network. Despite its simplicity and analytical tractability, PPP may not always be a suitable model for all spatial configurations of nodes. In the context of this paper, the locations of vehicular nodes and RSUs in vehicular networks are restricted to roadways, which are predominantly linear and randomly oriented. The 2D PPP model, in which the location of nodes are modeled by randomly distributed points in the 2D plane, does not capture the coupling between the nodes and the underlying infrastructure (roads) in vehicular networks. While modeling the locations of vehicular nodes, one has to consider two fundamental sources of *randomness*: (i) the locations of nodes on each road are often irregular and can hence be treated as a realization of a point process, and (ii) the layout of the roads is also often irregular, which makes it possible to model the road system as a realization of a line process [9]–[13]. In short, it is necessary to consider doubly stochastic spatial models for vehicular nodes that account for the randomness associated with the roads as well as the locations of nodes on these roads. A well-known *canonical* model in the literature that readily meets this requirement is a Cox process or doubly stochastic Poisson point process [14], [15], where the roads in a network are modeled by a Poisson line process (PLP) and the location of nodes on the roads are modeled by a 1D PPP. Despite the relevance of this canonical model in understanding the system-level performance of vehicular networks, its coverage analysis is still an open problem, which is the main focus of this paper. In particular, we develop tools to characterize serving distance as well as conditional interference power distributions, which collectively provide exact characterization of coverage probability and can also be readily applied to study many other aspects of vehicular networks.

A. Related Work

While there is a significant volume of literature pertaining to the analysis of vehicular networks using tools from stochastic geometry, the spatial models considered in these works are usually limited to a single road or an intersection of two roads [16]–[21]. Although such models are usually accurate for vehicular networks formed on a sparse layout of roads, such as freeways, they may not always be accurate in capturing the performance of vehicular networks in dense urban scenarios

The authors are with Wireless@VT, Department of ECE, Virginia Tech, Blacksburg, VA (email: {vishnucr, hdhillon}@vt.edu). The support of the US NSF (Grant IIS-1633363) is gratefully acknowledged. This work will be presented in part at the IEEE ICC, Kansas City, MO, 2018 [1]. Manuscript last updated: April 19, 2018.

with a dense distribution of roads. For instance, a signal-to-interference plus noise ratio (SINR) based analysis to compute the optimum transmission probability for vehicles on a single road, has been proposed in [16]. The trade-offs between the aggregate packet progress and spatial frequency reuse for multi-hop transmission between vehicles in a multi-lane highway setup were studied in [18]. In [20], [21], the authors have analyzed the packet reception probability of a link at the intersection of two perpendicular roads where the location of nodes are modeled as 1D PPP on each road. Since these models do not accurately capture the irregular layout of roads and their effect on the performance, they do not always offer reliable system-level insights that aid in the design.

Although relatively sparse, there are also a few works in the literature where more sophisticated models that include the randomness associated with the road systems were studied [9]–[13], [22], [23]. In [9], the authors have modeled the streets in an urban setting by a Manhattan Poisson line process (MPLP) and the base stations on each road by a 1D PPP and characterized the downlink coverage performance of mmWave microcells by adopting a Manhattan distance based path-loss model. While this is a reasonable model for mmWave communication in an urban setting, it may not be applicable to all scenarios due to the irregular structure of roads. A more refined model for vehicular networks is presented in [11], [12], where the streets are modeled by the edges of either a Poisson-Line tessellation (PLT), Poisson-Voronoi tessellation (PVT), or a Poisson-Delaunay tessellation (PDT) and the nodes on each line are modeled by a homogeneous 1D PPP. Owing to its analytical tractability, PLT often gains preference over PVT and PDT in modeling road systems (it has also been used in other related applications, such as in modeling the effect of blockages in localization networks [24]). In [11], the authors have considered a hierarchical two-tier network whose components are modeled as a Cox process on a PLT and have characterized the mean shortest path on the streets connecting these components. Using the same spatial model, a formula for probability density function of inter-node distances was presented in [12]. In [13], the author has derived the uplink coverage probability for a setup where the typical receiver is randomly chosen from a PPP and the locations of transmitter nodes are modeled as a Cox process driven by a PLP. However, to the best of our knowledge, this paper is the first to derive the coverage probability for a setup where both the receiver and transmitter nodes are modeled by Cox processes driven by the same PLP. In other words, this paper is the first to derive the coverage probability of a vehicular node located on a PLP when it connects to another vehicular node on the same PLP. The technical challenges in this analysis originate from the spatial coupling between the vehicular nodes induced by the underlying PLP. More detailed account of our contributions is provided below.

B. Contributions

In this paper, we present an analytical procedure for performing the canonical coverage analysis of a vehicular network. We consider a doubly-stochastic spatial model for wireless nodes, which captures the irregularity in the spatial layout of roads by modeling them as a PLP and the spatial irregularity in the locations of wireless nodes by modeling them as a 1D PPP on each road. In order to mimic various fading scenarios, we choose Nakagami-m fading channel that allows us to control the severity of fading. For this setup, we derive the signal-to-interference ratio (SIR) based coverage probability of a typical receiver, which is an arbitrarily chosen receiving node in the network, assuming that it connects to its closest transmitting node in the network. We then study the trends in the coverage performance which offers some design insights. More technical details about the coverage probability and system-level insights are provided next.

Coverage probability. We derive an exact expression for coverage probability by characterizing the interference experienced at the typical receiver. We first derive several fundamental distance distributions that are necessary to characterize the desired signal power at the typical receiver. Since the distribution of nodes is coupled with the distribution of lines in the network, it poses two key challenges to the exact coverage analysis. First, the serving node, which is the closest transmitting node to the typical receiver, can possibly be located on any of the lines in the network. Consequently, the interference measured at the typical receiver in each of these cases is different and we have to handle each case separately. In order to address this issue, we derive a generalized expression for coverage probability for all these cases. Second, when a transmitting node on a particular line is chosen to be the serving node, it implies that there can not be any line with a node whose distance to the typical receiver is smaller than the distance between the typical receiver and the serving node. This additional constraint imposed by the distribution of nodes impacts the conditional distribution of lines as observed at the typical receiver. We determine the conditional distribution of the lines in order to compute the interference at the typical receiver. We then determine the coverage probability in terms of derivative of Laplace transform of the distribution of the interference power. We also provide some theoretical insights by studying the asymptotic characteristics of coverage probability.

System-level insights. Using our analytical results, we study the effect of two key network parameters, namely, node density and line density, on the coverage probability of the typical receiver. We observe that the coverage probability increases as the density of nodes on lines increases. However, the coverage probability degrades as the density of the lines in the network increases. The contrasting effect of node and line densities on the coverage probability offers some insights in the design and deployment of RSUs in the network. We also study the impact of line and node densities on area spectral efficiency (ASE) of the network. We show that the areas with sparse distribution of roads require a denser deployment of RSUs as compared to the areas with dense roads to achieve the same ASE.

II. Mathematical Preliminary: Poisson Line Process

Since the PLP will be the main component of our model described in Section III, a basic knowledge of its construction

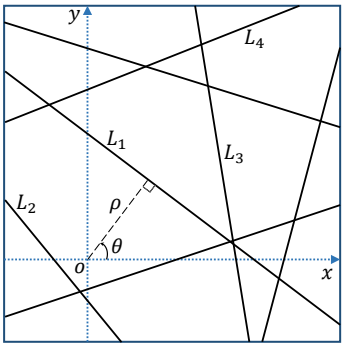

Fig. 1. Illustration of Poisson line process in two-dimensional plane $\mathbb{R}^2$.

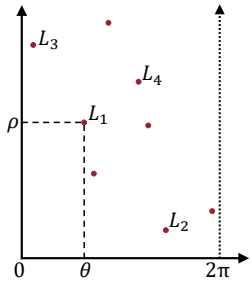

Fig. 2. Illustration of a point process on representation space $\mathcal{C} \equiv [0, 2\pi) \times [0, \infty)$.

and properties will be useful in understanding the proposed model. While we provide only a brief introduction to PLP and its properties in this section, a detailed account of the underlying theory can be found in [14], [25]. *Line process*. A line process is simply a random collection of lines in a 2D plane. Any undirected line L in $\mathbb{R}^2$ can be uniquely characterized by its perpendicular distance ρ from the origin $o \equiv (0, 0)$ and the angle θ subtended by the perpendicular dropped onto the line from the origin with respect to the positive x-axis in counter clockwise direction, as shown in Fig. 1. The pair of parameters ρ and θ can be represented as the coordinates of a point on the cylindrical surface $\mathcal{C} \equiv [0, 2\pi) \times [0, \infty)$, which is termed as the *representation space*, as illustrated in Fig. 2. Clearly, there is a one-to-one correspondence between the lines in $\mathbb{R}^2$ and points on the cylindrical surface $\mathcal{C}$. Thus, a random collection of lines can be constructed from a set of points on $\mathcal{C}$. Such a set of lines generated by a Poisson point process on $\mathcal{C}$ is called a Poisson line process. In our system model, we also assume the PLP to be motion-invariant for analytical simplicity. So, we will discuss the concept of motion-invariance for line processes and some well-established results of PLP next.

Stationarity and Motion-Invariance. The definition of stationarity for line processes is similar to that of point processes. A line process $\Phi_l = \{L_1, L_2, \dots\}$ is said to be stationary if the translated line process $T\Phi_l = \{T(L_1), T(L_2), \dots\}$ has the same distribution of lines as that of Φ_l for any translation T in the plane. Upon translating the origin in the plane $\mathbb{R}^2$ by a distance t in a direction that makes an angle β with respect to the positive x-axis, the equivalent representation of a line L in $\mathcal{C}$ changes from (ρ, θ) to $\big(\rho - t\cos(\theta - \beta), \theta\big)$. Therefore, for a stationary line process Φ_l, the point process $\big\{\big(\rho_{L_1} - t\cos(\theta_{L_1} - \beta), \theta_{L_1}\big), \big(\rho_{L_2} - t\cos(\theta_{L_2} - \beta), \theta_{L_2}\big), \dots\big\}$ in the representation space $\mathcal{C}$ has the same distribution as that of the point process $\big\{\big(\rho_{L_1}, \theta_{L_1}\big), \big(\rho_{L_2}, \theta_{L_2}\big), \dots\big\}$. Similarly, rotation of the axes about the origin by an angle γ in $\mathbb{R}^2$ changes the representation of the line in $\mathcal{C}$ from (ρ, θ) to $(\rho, \theta - \gamma)$, where the operation $\theta - \gamma$ is modulo 2π. In addition to translation-invariance, if a line process is also invariant to the rotation of the axes about the origin, then it is said to be motion-invariant.

Line density. Line density μ of a line process Φ_l is defined as the mean line length per unit area. If Φ_l is a motion-invariant line process, then the density of the corresponding point process λ in the representation space $\mathcal{C}$ is given by $\lambda = \frac{\mu}{\pi}$.

Number of lines intersecting a disc. If Φ_l is a motion-invariant Poisson line process with line density μ, then the number of lines that intersect a convex region $K \subseteq \mathbb{R}^2$ follows a Poisson distribution with mean

$$\tau_K = \frac{\mu\nu(K)}{\pi} = \lambda\nu(K), \tag{1}$$

where $\nu(K)$ is the perimeter of the convex region K. Therefore, the number of lines intersecting a disc of radius d is Poisson distributed with mean $2\pi\lambda d$.

III. System Model

A. Spatial Modeling of Wireless Nodes

We first model the spatial distribution of road systems by a motion-invariant PLP Φ_l with line density μ_l. We denote the density of equivalent PPP on the representation space $\mathcal{C}$ by λ_l. We then model the locations of wireless nodes, which include vehicular nodes and RSUs, on each line (road) by a homogeneous 1D PPP with density λ_n. We assume a slotted ALOHA channel access scheme. It should be noted that this scheme is also a reasonable approximation for carrier-sense multiple access (CSMA) scheme for vehicular networks in the regimes of high and low node densities [26], [27]. Assuming that each node transmits with a probability p, the location of transmitting nodes on each line is then given by a thinned PPP with density $\lambda_v = p\lambda_n$. We denote the set of locations of the transmitting nodes on a line L by $\{\mathbf{w}_L\} \equiv \Psi_L$. Similarly, the distribution of receiving nodes on each line is also a thinned PPP with density $\lambda_r = (1 - p)\lambda_n$. Thus, the locations of transmitting and receiving nodes are modeled by Cox processes Φ_t and Φ_r, which are driven by the same PLP Φ_l. Our goal is to derive the SIR based coverage probability of a typical receiver from the point process Φ_r. For analytical simplicity, we translate the origin $o \equiv (0, 0)$ to the location of the typical receiver. The translated point process Φ_{r_0} can be treated as the superposition of the point process Φ_r, an independent 1D PPP with density λ_r on a line passing through the origin, and an atom at the origin o [13]. This can be understood by applying Slivnyak's theorem [14], [15] in two steps: first, we add a point at the origin to the PPP in the representation space $\mathcal{C}$, thereby obtaining

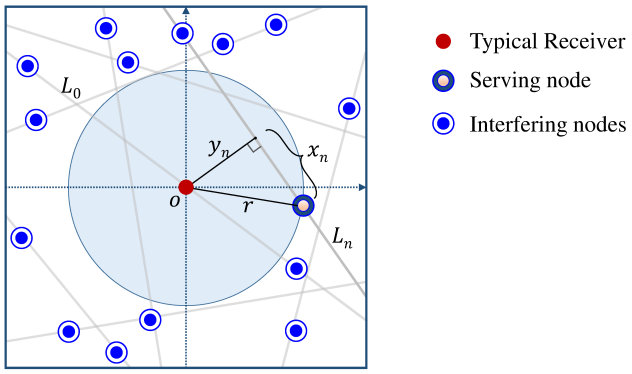

Fig. 3. Illustration of the system model.

a PLP $\Phi_{l_0} = \Phi_l \cup \{L_0\}$ with a line L_0 passing through the origin, and second, we add a point at the origin to the 1D-PPP on the line L_0 passing through the origin in $\mathbb{R}^2$. The line L_0 passing through the origin will henceforth be referred to as the typical line. Since both Φ_r and Φ_t are driven by the same line process, the translated point process Φ_{t_0} is also the superposition of Φ_t and an independent PPP with density λ_v on L_0, as shown in Fig. 3. Since the other receiver nodes in the network do not have any impact on the SIR measured at the typical receiver in this setup, we will focus only on the distribution of transmitter nodes in the network. For brevity, the transmitter nodes will henceforth be referred to as only *nodes*. We denote the i^{th} $(i = 1, 2, \dots)$ closest line to the origin o (excluding the typical line) by L_i and its perpendicular distance to the origin by Y_i. The distance of the closest node on a line L_i from the projection of the origin onto L_i is denoted by X_i, as illustrated in Fig. 3. Thus, the distance to the closest node on L_i from the origin is $S_i = \sqrt{Y_i^2 + X_i^2}$. For notational consistency, we denote the distance of the typical line from the origin by $Y_0 \equiv 0$ and the distance to the closest node on L_0 by S_0. We denote the number of lines that intersect a region $A \subset \mathbb{R}^2$ by $N_l(A)$ and the number of nodes in A by $N_v(A)$. Throughout this paper, we denote the random variables by upper case letters and their corresponding realizations by lower case letters. For instance, Y_n denotes a random variable, whereas y_n denotes its realization.

B. Transmitter Association Scheme and Propagation Model

We assume that the transmit power is the same for all the nodes and the antennas are isotropic. We further assume that the typical receiver connects to its closest transmitting node in the network. Note that the closest node does not necessarily have to be on the same line as that of the typical receiver and can possibly be located on any of the other lines. We denote such an event in which the serving node is located on the i^{th} closest line (excluding the typical line) to the origin by $\mathcal{E}_i$ $(i = 1, 2, \dots)$. We denote the event in which the serving node is located on the typical line by $\mathcal{E}_0$.

In wireless communication networks, the severity of fading between the transmitter and the receiver depends on environmental factors and hence, the effect of fading can vary significantly from an urban scenario consisting of several buildings to rural areas and highways which are almost devoid of any tall structures. Therefore, in order to mimic a wide range of fading environments, we choose Nakagami-m fading. Also, the severity of fading of the communication links between the typical receiver and the nodes located on the typical line differs from that of the links between the typical receiver and the nodes located on other lines. So, we denote the fading parameters for these two types of links by m_0 and m, respectively. In the interest of analytical tractability, we restrict the values of m_0 and m to integers. For simplicity of exposition, we assume that the system is interference limited and hence, the thermal noise is neglected. Thus, the signal-to-interference ratio (SIR) at the typical receiver is

$$\texttt{SIR} = \frac{G_0 R^{-\alpha}}{\sum_{L_j \in \Phi_{l_0}} \sum_{\mathrm{w}_{L_j} \in \Psi_{L_j} \setminus b(o,R)} G_{\mathrm{w}_{L_j}} \|\mathrm{w}_{L_j}\|^{-\alpha}}, \tag{2}$$

where $\alpha > 2$ is the path-loss exponent, G_0 is the channel fading gain between the typical receiver and the serving node, $G_{\mathrm{w}_{L_j}}$ is the channel fading gain between the typical receiver and the interfering node at the location w_{L_j}, R is the Euclidean distance to the serving node from the typical receiver, and $\|\mathrm{w}_{L_j}\|$ is the Euclidean distance of the interfering node from the typical receiver. The notation followed in this paper is summarized in Table I.

IV. Coverage Probability

This is the main technical section of the paper, where we derive the coverage probability for the setup described in the previous section. Recall that the serving node which is the closest node to the typical receiver can possibly be located on any line L_k $(k = 0, 1, \dots)$. As a result, the interference at the typical receiver will be different in each of these cases and hence, they need to be handled separately. However, we can derive a generalized expression for the cases in which the serving node does not lie on the typical line ($\mathcal{E}_1$, $\mathcal{E}_2$, ...). Therefore, in our analysis, we will derive the coverage probability conditioned on the events $\mathcal{E}_0$ and $\mathcal{E}_n$ $(n = 1, 2, \dots)$ separately and obtain the final result using law of total probability. A key difference between the events $\mathcal{E}_0$ and $\mathcal{E}_n$ is that the distance of the line on which the serving node is located is always zero in case of $\mathcal{E}_0$, whereas the distance of the line containing the serving node Y_n in case of $\mathcal{E}_n$ is a random variable. Therefore, in the computation of coverage probability conditioned on $\mathcal{E}_n$, we will derive the intermediate results by additionally conditioning on Y_n. In the final step, we obtain the overall coverage probability by taking expectation over Y_n. While we can obtain some of the results for the case $\mathcal{E}_0$ from the intermediate results pertaining to $\mathcal{E}_n$ by simply substituting $Y_0 = 0$ in place of Y_n, we will provide detailed proofs for those results where this approach is not applicable.

A. Preliminary Results

We begin our analysis with the derivation of some fundamental distance distributions which will be used later in the computation of coverage probability. While it may be

TABLE I
SUMMARY OF NOTATION

Notation	Description
Φ_l; Φ_{l_0}	Poisson line process; The line process Φ_l plus a line passing through the origin $o \equiv (0,0)$
μ_l; λ_l	Line density of the PLP Φ_l; The density of equivalent PPP of Φ_l in the representation space $\mathcal{C}$
λ_v; λ_r	Density of transmitting nodes on each line; Density of receiving nodes on each line
$\{\mathbf{w}_L\} \equiv \Psi_L$	Set of locations of transmitting nodes on a line L
L_0; L_n	Line passing through the origin o (Typical line); The n^{th} closest line to the origin
Y_i; X_i	Distance of the i^{th} close line from o; Distance of the closest node on L_i from the projection of the origin onto L_i
S_i	Distance of the closest node on L_i from the typical receiver at the origin
R	Distance between the typical receiver and the serving node
G_0; G_i	Channel fading gain of the serving link; Channel fading gain of i^{th} interfering link
$\mathcal{E}_0$; $\mathcal{E}_i$	Event that the serving node is located on the typical line L_0; Event that the serving node is located on L_i
β; $\mathtt{P_c}$; $\mathtt{ASE}$	SIR threshold; Coverage probability; Area spectral efficiency

relatively straightforward to derive some of these results, they are presented here for completeness.

Lemma 1. *The cumulative distribution function (CDF) and probability density function (PDF) of the distance of the n^{th} closest line from the origin Y_n are*

$$\textit{CDF:}\quad F_{Y_n}(y_n) = 1 - e^{-2\pi\lambda_l y_n}\sum_{k=0}^{n-1}\frac{(2\pi\lambda_l y_n)^k}{k!},$$
$$\textit{PDF:}\quad f_{Y_n}(y_n) = \frac{e^{-2\pi\lambda_l y_n}(2\pi\lambda_l y_n)^n}{y_n(n-1)!}. \tag{3}$$

Proof: From the definition of a PLP, recall that there is a one-to-one correspondence between lines in $\mathbb{R}^2$ and points on $\mathcal{C} \equiv [0\ 2\pi) \times [0\ \infty)$. The abscissa and the ordinate of these points represent the orientation of the line and the distance of the line from the origin, respectively. We now consider the projections of these points onto the vertical axis of the cylindrical surface, which represents the distance of the lines from the origin. Note that the number of projections of points in a segment of length t on the vertical axis of $\mathcal{C}$ is the same as the number of points in the area $[0, 2\pi) \times [0, t)$, which follows a Poisson distribution with mean $2\pi\lambda_l t$. This means that the projections of points onto the vertical axis of $\mathcal{C}$ forms a 1D PPP Ψ_{l_0} with density $2\pi\lambda_l$. Therefore, the distance of the n^{th} closest line from the origin follows the same distribution as that of the distance of n^{th} closest point in a 1D PPP with density $2\pi\lambda_l$, which is a well-known result in stochastic geometry [15]. ∎

Lemma 2. *Conditioned on the distance of the n^{th} closest line to the origin Y_n, the CDF of the distance X_n between the projection of origin onto the line L_n and its closest node on L_n is*

$$F_{X_n}(x_n|y_n) = 1 - \exp(-2\lambda_v x_n). \tag{4}$$

Proof: The proof follows from the void probability of a 1D PPP with density λ_v. ∎

Lemma 3. *Conditioned on the distance of the n^{th} closest line to the origin Y_n, the CDF and PDF of the distance to the closest node on the line L_n from the typical receiver S_n are*

$$\textit{CDF:}\quad F_{S_n}(s_n|y_n) = 1 - e^{-2\lambda_v\sqrt{s_n^2-y_n^2}},$$
$$\textit{PDF:}\quad f_{S_n}(s_n|y_n) = \frac{2\lambda_v s_n}{\sqrt{s_n^2-y_n^2}}e^{-2\lambda_v\sqrt{s_n^2-y_n^2}}. \tag{5}$$

Proof: The conditional CDF of S_n is given by

$$\begin{aligned}F_{S_n}(s_n|y_n) &= \mathbb{P}(S_n < s_n|Y_n) = \mathbb{P}(\sqrt{X_n^2+y_n^2} < s_n|Y_n)\\ &= \mathbb{P}(X_n < \sqrt{s_n^2-y_n^2}|Y_n) = F_{X_n}(\sqrt{s_n^2-y_n^2}|y_n)\\ &= 1-\exp(-2\lambda_v\sqrt{s_n^2-y_n^2}).\end{aligned}$$

The PDF $f_{S_n}(s_n|y_n)$ can be obtained by taking the derivative of $F_{S_n}(s_n|y_n)$ w.r.t. s_n. ∎

Corollary 1. *The CDF and the PDF of the distance between the typical receiver at the origin and its closest node on the typical line S_0 are*

$$\textit{CDF:}\quad F_{S_0}(s_0) = 1 - \exp(-2\lambda_v s_0),$$
$$\textit{PDF:}\quad f_{S_0}(s_0) = 2\lambda_v \exp(-2\lambda_v s_0). \tag{6}$$

Proof: The proof follows from replacing S_n and Y_n with S_0 and $Y_0 = 0$ in Lemma 3. ∎

Conditioned on the distance Y_n, we will now derive the distribution of the distance of the closest node to the typical receiver among the nodes that are located on the lines that are closer and farther than the line of interest L_n in the following Lemmas. These results will be used in the next subsection in the computation of the probability of occurrence of events $\mathcal{E}_0$ and $\mathcal{E}_n$.

Lemma 4. *Conditioned on the distance of the n^{th} closest line to the origin Y_n, the CDF and PDF of the distance U_n between the typical receiver and its closest node among the $n-1$ lines $\{L_1, L_2, \ldots L_{n-1}\}$ (excluding the typical line) that are closer than Y_n are*

$$\textit{CDF:}\quad F_{U_n}(u_n|y_n) =$$
$$\begin{cases}1-\left(1-\dfrac{u_n}{y_n}+\dfrac{1}{y_n}\displaystyle\int_0^{u_n} g(u_n,z)\mathrm{d}z\right)^{n-1}, & 0 \le u_n < y_n,\\ 1-\left(\displaystyle\int_0^{y_n} g(u_n,z)\frac{\mathrm{d}z}{y_n}\right)^{n-1}, & y_n \le u_n < \infty,\end{cases}$$
$$\textit{PDF:}\quad f_{U_n}(u_n|y_n) =$$

$$\begin{cases} (n-1)\Big(1-\dfrac{u_n}{y_n}+\displaystyle\int_0^{u_n} g(u_n,z)\frac{\mathrm{d}z}{y_n}\Big)^{n-2} \\ \qquad \times\Big(\displaystyle\int_0^{u_n}\frac{2\lambda_v u_n g(u_n,z)}{y_n\sqrt{u_n^2-z^2}}\mathrm{d}z\Big), & 0\le u_n<y_n, \\ (n-1)\Big(\displaystyle\int_0^{y_n}\frac{2\lambda_v u_n g(u_n,z)}{y_n\sqrt{u_n^2-z^2}}\mathrm{d}z\Big) \\ \qquad \times\Big(\displaystyle\int_0^{y_n} g(u_n,z)\frac{\mathrm{d}z}{y_n}\Big)^{n-2}, & y_n\le u_n<\infty, \end{cases} \tag{7}$$

where $g(u_n,z)=\exp(-2\lambda_v\sqrt{u_n^2-z^2})$.

Proof: See Appendix A. ∎

Lemma 5. *Conditioned on the distance of the n^{th} closest line to the origin Y_n, the CDF and PDF of the distance V_n between the typical receiver and its closest node among the lines $\{L_{n+1}, L_{n+2}, \dots\}$ that are farther than Y_n are*

$$\textit{CDF: } F_{V_n}(v_n|y_n)=1-\exp\Big[-2\pi\lambda_l\int_{y_n}^{v_n}1-e^{-2\lambda_v\sqrt{v_n^2-z^2}}\mathrm{d}z\Big], \quad y_n\le v_n<\infty, \tag{8}$$

$$\textit{PDF: } f_{V_n}(v_n|y_n)=2\pi\lambda_l\int_{y_n}^{v_n}e^{-2\lambda_v\sqrt{v_n^2-z^2}}\frac{2\lambda_v v_n}{\sqrt{v_n^2-z^2}}\mathrm{d}z \times\exp\Big[-2\pi\lambda_l\int_{y_n}^{v_n}1-e^{-2\lambda_v\sqrt{v_n^2-z^2}}\mathrm{d}z\Big], \quad y_n\le v_n<\infty. \tag{9}$$

Proof: See Appendix B. ∎

We can easily specialize the results of Lemma 5 to obtain the CDF and PDF of the distance between the typical receiver and its closest node among the lines that are farther than the typical line as given in the following Corollary.

Corollary 2. *The CDF and PDF of the distance V_0 between the typical receiver and its closest node among the lines that are farther than the typical line are*

$$\textit{CDF: } F_{V_0}(v_0)=1-\exp\Big[-2\pi\lambda_l\int_0^{v_0}1-e^{-2\lambda_v\sqrt{v_0^2-z^2}}\mathrm{d}z\Big], \tag{10}$$

$$\textit{PDF: } f_{V_0}(v_0)=2\pi\lambda_l\int_0^{v_0}e^{-2\lambda_v\sqrt{v_0^2-z^2}}\frac{2\lambda_v v_0}{\sqrt{v_0^2-z^2}}\mathrm{d}z \times\exp\Big[-2\pi\lambda_l\int_0^{v_0}1-e^{-2\lambda_v\sqrt{v_0^2-z^2}}\mathrm{d}z\Big]. \tag{11}$$

Proof: The proof follows from replacing V_n and Y_n with V_0 and $Y_0=0$ in Lemma 5. ∎

B. Probabilities of Events $\mathcal{E}_n$ and $\mathcal{E}_0$

In this subsection, we will derive the probability with which the typical receiver connects to a node on the n^{th} closest line to the origin conditioned on the distance of the line from the origin Y_n and the probability with which the typical receiver connects to a node on the typical line. These intermediate results hold the key to the derivation of conditional serving distance distribution in the next subsection.

Lemma 6. *Conditioned on Y_n, the probability of occurrence of the event $\mathcal{E}_n$ is*

$$\mathbb{P}(\mathcal{E}_n|Y_n)=\int_0^{\infty}\Big(1-F_{S_0}(s_n)\Big)\Big(1-F_{U_n}(s_n|y_n)\Big)\times\Big(1-F_{V_n}(s_n|y_n)\Big)f_{S_n}(s_n|y_n)\mathrm{d}s_n, \tag{12}$$

where $F_{S_0}(\cdot)$, $F_{U_n}(\cdot\ |y_n)$, $F_{V_n}(\cdot|y_n)$, and $f_{S_n}(s_n|y_n)$ are given by Corollary 1, Lemmas 4, 5, and 3, respectively.

Proof: The typical receiver connects to a node on the n^{th} closest line if the distance to the closest node on the line L_n is smaller than the distance to the closest node on any other line. In this case, we will group all the lines excluding the line of interest L_n into 3 sets: (i) the typical line L_0, (ii) the lines that are closer than the line L_n (L_1, L_2, …, L_{n-1}), and (iii) the lines that are farther than the line L_n (L_{n+1}, L_{n+2}, …). The distance to the closest node on L_n must be smaller than the distance to the closest node in each of these three sets, i.e., S_n must be smaller than the minimum of S_0, U_n, and V_n. Thus, the conditional probability of occurrence of the event $\mathcal{E}_n$ is computed as

$$\begin{aligned}\mathbb{P}(\mathcal{E}_n|Y_n)&=\mathbb{P}(S_n<\min\{S_0,U_n,V_n\}|Y_n)\\&=\mathbb{P}(S_n<S_0,S_n<U_n,S_n<V_n|Y_n)\\&\overset{(a)}{=}\int_0^{\infty}\mathbb{P}(S_0>s_n|S_n,Y_n)\mathbb{P}(U_n>s_n|S_n,Y_n)\times\mathbb{P}(V_n>s_n|S_n,Y_n)f_{S_n}(s_n|y_n)\mathrm{d}s_n\\&\overset{(b)}{=}\int_0^{\infty}\Big(1-F_{S_0}(s_n)\Big)\Big(1-F_{U_n}(s_n|y_n)\Big)\times\Big(1-F_{V_n}(s_n|y_n)\Big)f_{S_n}(s_n|y_n)\mathrm{d}s_n,\end{aligned}$$

where (a) follows from the conditional independence of the variables S_0, U_n, and V_n, and (b) follows from the independence of the random variable S_0. ∎

Corollary 3. *The probability of occurrence of the event $\mathcal{E}_0$ is*

$$\mathbb{P}(\mathcal{E}_0)=\int_0^{\infty}(1-F_{V_0}(s_0))f_{S_0}(s_0)\mathrm{d}s_0, \tag{13}$$

where $F_{V_0}(\cdot)$ and $f_{s_0}(\cdot)$ are given by Corollaries 1 and 2, respectively.

Proof: The typical receiver at the origin connects to a node on the typical line when the distance to the closest node on the typical line is smaller than the distance to the closest node on any other line. Thus, the probability of occurrence of $\mathcal{E}_0$ is given by

$$\begin{aligned}&\mathbb{P}(\mathcal{E}_0)=\mathbb{P}(S_0<\min\{S_1,S_2,\dots\})=\mathbb{P}(S_0<V_0)\\&=\int_0^{\infty}\mathbb{P}(V_0>s_0|S_0)f_{S_0}(s_0)\mathrm{d}s_0=\int_0^{\infty}(1-F_{V_0}(s_0))f_{S_0}(s_0)\mathrm{d}s_0,\end{aligned}$$

which completes the proof. ∎

C. Serving Distance Distribution

In this subsection, we will derive the distribution of distance between the typical receiver and the serving node conditioned on the events $\mathcal{E}_n$ and $\mathcal{E}_0$. As stated in the previous subsection, in case of $\mathcal{E}_n$, the distance to the closest node on the n^{th}

closest line S_n must be smaller than the minimum of S_0, U_n, and V_n. Therefore, we first determine the distribution of $W_n = \min\{S_0, U_n, V_n\}$ in the following Lemma.

Lemma 7. *Conditioned on the distance of the n^{th} closest line to the origin Y_n, the CDF and PDF of $W_n = \min\{S_0, U_n, V_n\}$ are*

$$\textit{CDF: } F_{W_n}(w_n|y_n) = 1-\big(1-F_{S_0}(w_n)\big)\big(1-F_{U_n}(w_n|y_n)\big)\big(1-F_{V_n}(w_n|y_n)\big), \quad (14)$$

$$\textit{PDF: } f_{W_n}(w_n|y_n) = f_{S_0}(w_n)\big(1-F_{U_n}(w_n|y_n)\big)\big(1-F_{V_n}(w_n|y_n)\big) + \big(1-F_{S_0}(w_n)\big)f_{U_n}(w_n|y_n)\big(1-F_{V_n}(w_n|y_n)\big) + \big(1-F_{S_0}(w_n)\big)\big(1-F_{U_n}(w_n|y_n)\big)f_{V_n}(w_n|y_n), \quad (15)$$

where $F_{S_0}(\cdot)$, $f_{S_0}(\cdot)$ are given by Corollary 1, $F_{U_n}(\cdot\ |y_n)$, $f_{U_n}(\cdot\ |y_n)$ are given by Lemma 4, and $F_{V_n}(\cdot|y_n)$, $f_{V_n}(\cdot|y_n)$ are given by Lemma 5.

Proof: The proof simply follows from the distribution of minimum of three independent random variables [28]. ∎

Using the intermediate results derived thus far, we will now derive the conditional distribution of the serving distance R in the following Lemma.

Lemma 8. *Conditioned on the event $\mathcal{E}_n$ and the distance of the n^{th} closest line Y_n, the CDF and PDF of the serving distance R are*

$$\textit{CDF: } F_R(r|\mathcal{E}_n, Y_n) = 1 - \frac{1}{\mathbb{P}(\mathcal{E}_n|Y_n)} \times \int_r^\infty \big(F_{S_n}(w_n|y_n) - F_{S_n}(r|y_n)\big) f_{W_n}(w_n|y_n)\mathrm{d}w_n, \quad (16)$$

$$\textit{PDF: } f_R(r|\mathcal{E}_n, y_n) = \int_r^\infty \frac{f_{S_n}(r|y_n) f_{W_n}(w_n|y_n)}{\mathbb{P}(\mathcal{E}_n|Y_n)}\mathrm{d}w_n, \quad (17)$$

where $F_{S_n}(\cdot|y_n)$, $f_{S_n}(\cdot|y_n)$ are given by Lemma 3, $\mathbb{P}(\mathcal{E}_n|Y_n)$ and $f_{W_n}(\cdot|y_n)$ are given by Lemmas 6 and 7, respectively.

Proof: The conditional CDF of the serving distance R is computed as

$$\begin{aligned} F_R(r|\mathcal{E}_n, Y_n) &= 1-\mathbb{P}(R > r|\mathcal{E}_n, Y_n) = 1-\frac{\mathbb{P}(R > r, \mathcal{E}_n|Y_n)}{\mathbb{P}(\mathcal{E}_n|Y_n)} \\ &\overset{(a)}{=} 1 - \frac{\mathbb{P}(S_n > r, S_n < \min\{S_0, U_n, V_n\}|Y_n)}{\mathbb{P}(\mathcal{E}_n|Y_n)} \\ &= 1 - \frac{\mathbb{P}(r < S_n < W_n|Y_n)}{\mathbb{P}(\mathcal{E}_n|Y_n)} \\ &= 1 - \int_r^\infty \frac{\mathbb{P}(r < S_n < w_n|W_n, Y_n)}{\mathbb{P}(\mathcal{E}_n|Y_n)} f_{W_n}(w_n|y_n)\mathrm{d}w_n \\ &= 1 - \int_r^\infty \frac{\big(F_{S_n}(w_n|y_n) - F_{S_n}(r|y_n)\big)}{\mathbb{P}(\mathcal{E}_n|Y_n)} f_{W_n}(w_n|y_n)\mathrm{d}w_n, \end{aligned}$$

where (a) follows from the condition for the occurrence of the event $\mathcal{E}_n$. The conditional PDF $f_R(r|\mathcal{E}_n, y_n)$ can be computed by taking the derivative of $F_R(r|\mathcal{E}_n, y_n)$ w.r.t. r. ∎

Lemma 9. *Conditioned on the event $\mathcal{E}_0$, the CDF and PDF of the serving distance R are given by*

$$\textit{CDF: } F_R(r|\mathcal{E}_0) = 1 - \int_r^\infty \frac{\big(F_{S_0}(v_0) - F_{S_0}(r)\big)}{\mathbb{P}(\mathcal{E}_0)} f_{V_0}(v_0)\mathrm{d}v_0, \quad (18)$$

$$\textit{PDF: } f_R(r|\mathcal{E}_0) = \frac{1}{\mathbb{P}(\mathcal{E}_0)} \int_r^\infty f_{S_0}(r) f_{V_0}(v_0)\mathrm{d}v_0, \quad (19)$$

where $F_{S_0}(\cdot)$, $f_{S_0}(\cdot)$ are given by Corollary 1, $f_{V_0}(v_0)$ and $\mathbb{P}(\mathcal{E}_0)$ are given by Corollaries 2 and 3, respectively.

Proof: The proof follows along the same lines as that of Lemma 8. ∎

D. Conditional Probability Mass Function of Number of Lines

Now that we have derived the distribution of the serving distance R, the next main step is to characterize the interference experienced at the typical receiver conditioned on R for the events $\mathcal{E}_n$ and $\mathcal{E}_0$. The sources of interference are all the nodes that are located at a distance farther than R from the origin, i.e., the nodes that lie outside the disc $b(o, R)$ centered at the origin o with radius R. Please note that such nodes could also lie on lines which are located closer than R. Please see Fig. 4 for an illustration. Therefore, in order to characterize the interference, we will have to first determine the distribution of lines. In order to explain this concretely, let us consider the case of $\mathcal{E}_n$, where the serving node is located at a distance R on the n^{th} closest line from the origin. From the properties of PLP, we know that the number of lines intersecting a disc of fixed radius follows a Poisson distribution with mean equal to the line density scaled by the perimeter of the disc. However, this does not hold for the *conditional distribution* of the number of lines that intersect the disc $b(o, R)$. This is because the lines that intersect the disc $b(o, R)$ must not contain any nodes in the chord segment inside the disc (since we have already conditioned on the event that the serving node is located on L_n at a distance R from the typical receiver). This additional constraint imposed by the distribution of nodes on the lines impacts the conditional distribution of number of lines intersecting the disc $b(o, R)$. Note that the typical line is not included in the count of number of lines intersecting the disc $b(o, R)$. Now, conditioned on the event $\mathcal{E}_n$, we know that there are at least n lines that intersect the disc $b(o, R)$ which include the $n-1$ lines that are closer than the line of interest L_n and the line L_n itself which is at a distance $Y_n \leq R$. In addition to these n lines, there are also a random number of lines that are farther than Y_n but closer than the serving distance R, as illustrated in Fig. 4. Therefore, our immediate goal is to determine the conditional distribution of this random number of lines that intersect the disc $b(o, R)$ but do not intersect the disc $b(o, Y_n)$, denoted by $N_l\big(b(o, R) \setminus b(o, Y_n)\big)$.

Lemma 10. *Conditioned on the event $\mathcal{E}_n$, the distance of the n^{th} closest line Y_n, and the serving distance R, the probability mass function (PMF) of number of lines that are farther than Y_n and closer than R is*

$$\mathbb{P}\Big(N_l\big(b(o, r) \setminus b(o, y_n)\big) = k|\mathcal{E}_n, Y_n, R\Big) = \exp\left[-2\pi\lambda_l \int_{y_n}^{r} e^{-2\lambda_v\sqrt{r^2-y^2}}\mathrm{d}y\right] \frac{\left[2\pi\lambda_l \int_{y_n}^{r} e^{-2\lambda_v\sqrt{r^2-y^2}}\mathrm{d}y\right]^k}{k!}. \quad (20)$$

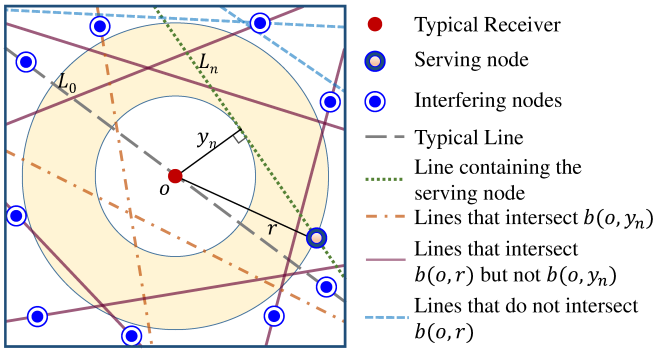

Fig. 4. Illustration of different sets of lines.

Proof: See Appendix C. ∎

Remark 1. *Conditioned on the event $\mathcal{E}_n$, serving distance R, and the distance of the n^{th} closest line to the origin Y_n, we have derived the PMF of number of lines that are farther than Y_n and closer than R. However, it can be observed that the conditional distribution remains Poisson but with a mean of $2\pi\lambda_l \int_{y_n}^{r} \exp(-2\lambda_v\sqrt{r^2-y^2})\mathrm{d}y$. Therefore, the conditional distribution of lines can be interpreted as a thinned Poisson line process with line density $\frac{\mu_l}{2\pi(r-y_n)} \int_{y_n}^{r} \exp\big(-2\lambda_v\sqrt{r^2-y^2}\big)\mathrm{d}y$.*

Corollary 4. *Conditioned on the event $\mathcal{E}_0$ and the serving distance R, the PMF of number of lines (excluding the typical line) that are closer than R is $\mathbb{P}(N_l(b(o,R)) = k|R,\mathcal{E}_0) =$*

$$\exp\left[-2\pi\lambda_l \int_0^r e^{-2\lambda_v\sqrt{r^2-y^2}}\mathrm{d}y\right] \frac{\left[2\pi\lambda_l \int_0^r e^{-2\lambda_v\sqrt{r^2-y^2}}\mathrm{d}y\right]^k}{k!}. \tag{21}$$

Proof: The proof follows from substituting $\mathcal{E}_0$ and $Y_0 = 0$ for $\mathcal{E}_n$ and Y_n in Lemma 10. ∎

E. Laplace Transform of Interference Distribution

In this subsection, we will determine the Laplace transform of the distribution of the interference power conditioned on the serving distance R. We will first consider the case where the typical receiver connects to the n^{th} closest line to the origin. In this case, we group the sources of interference into the following five sets: (i) the set of nodes present on the typical line, (ii) the set of nodes present on the line that contains the serving node which is at a distance Y_n, (iii) the set of nodes present on the lines that are closer than Y_n (excluding the typical line), (iv) the set of nodes present on the lines that are farther than Y_n but closer than the serving distance R (an annular region), and (v) the set of nodes present on the lines whose distance from the origin exceeds the serving distance R. We denote the interference from these five sets of nodes by I_0, I_n, I_{in}, I_{ann}, and I_{out}, respectively. We will now derive the Laplace transform of distribution of interference from each of these components.

The interference measured at the typical receiver from the nodes on the typical line is given by $I_0 = \sum_{\mathrm{w}_{L_0}\in\Psi_{L_0}\setminus b(o,R)} G_{\mathrm{w}_{L_0}} \|\mathrm{w}_{L_0}\|^{-\alpha}$, where Ψ_{L_0} is the 1-D PPP on the typical line, $G_{\mathrm{w}_{L_0}}$ are the channel gains between the typical receiver and the interfering nodes at w_{L_0}. While the Laplace transform of distribution of interference from nodes of a 1D PPP is very well-known, we still present the result in the following Lemma for completeness.

Lemma 11. *Conditioned on the event $\mathcal{E}_n$, serving distance R, and the distance of the n^{th} closest line Y_n, the Laplace transform of distribution of interference from the nodes situated on the typical line L_0 is*

$$\mathcal{L}_{I_0}(s|r,y_n,\mathcal{E}_n) = \exp\left[-2\lambda_v \int_r^\infty 1-\left(1+\frac{sx^{-\alpha}}{m_0}\right)^{-m_0}\mathrm{d}x\right]. \tag{22}$$

Proof: The distribution of nodes on the typical line is independent of the distance of the n^{th} closest line Y_n. Thus, the Laplace transform of distribution of interference from nodes on the typical line can be computed as

$$\begin{aligned}\mathcal{L}_{I_0}(s|r,y_n,\mathcal{E}_n) &= \mathbb{E}[e^{-sI_0}] \\ &= \mathbb{E}\,\mathbb{E}_G\left[\prod_{\mathrm{w}_{L_0}\in\Psi_{L_0}\setminus b(o,R)} \exp\left(-sG_{\mathrm{x}_{L_0}}\|\mathrm{w}_{L_0}\|^{-\alpha}\right)\right] \\ &\overset{(a)}{=} \mathbb{E}\left[\prod_{\mathrm{w}_{L_0}\in\Psi_{L_0}\setminus b(o,R)} \left(1+\frac{s\|\mathrm{w}_{L_0}\|^{-\alpha}}{m_0}\right)^{-m_0}\right] \\ &\overset{(b)}{=} \exp\left[-2\lambda_v \int_r^\infty \left(1-\left(1+\frac{sx^{-\alpha}}{m_0}\right)^{-m_0}\right)\mathrm{d}x\right],\end{aligned}$$

where (a) follows from the Gamma distribution of channel fading gains, and (b) follows from the PGFL of PPP and substituting $x = \|\mathrm{w}_{L_0}\|$. ∎

Lemma 12. *Conditioned on the event $\mathcal{E}_n$, the serving distance R, and the distance of the n^{th} closest line form the origin Y_n, the Laplace transform of distribution of interference from the nodes on the line L_n is*

$$\mathcal{L}_{I_n}(s|r,y_n,\mathcal{E}_n) = \exp\left[-2\lambda_v \int_{\sqrt{r^2-y_n^2}}^\infty 1-\left(1+\frac{s(x^2+y_n^2)^{-\alpha/2}}{m}\right)^{-m}\mathrm{d}x\right]. \tag{23}$$

Proof: The proof follows along the same lines as that of Lemma 11. ∎

Lemma 13. *Conditioned on the event $\mathcal{E}_n$, serving distance R, and the distance of the n^{th} closest line Y_n, the Laplace transform of distribution of interference from the nodes located on the lines that are closer than Y_n is*

$$\mathcal{L}_{I_{in}}(s|r,y_n,\mathcal{E}_n) = \left[\int_0^{y_n} \exp\left[-2\lambda_v \int_{\sqrt{r^2-y^2}}^\infty 1-\left(1+\frac{s(x^2+y^2)^{-\frac{\alpha}{2}}}{m}\right)^{-m}\mathrm{d}x\right]\frac{\mathrm{d}y}{y_n}\right]^{n-1}. \tag{24}$$

Proof: See Appendix D. ∎

Lemma 14. *Conditioned on the event $\mathcal{E}_n$, serving distance R, and the distance of the n^{th} closest line from the origin Y_n, the Laplace transform of distribution of interference from the nodes located on the lines that are farther than Y_n and closer than R is*

$$\mathcal{L}_{I_{ann}}(s|r,y_n,\mathcal{E}_n) = \exp\left[\left(-2\pi\lambda_l\int_{y_n}^{r} e^{-2\lambda_v\sqrt{r^2-z^2}}\mathrm{d}z\right)\left(1-\int_{y_n}^{r}\exp\left[-2\lambda_v \times \int_{\sqrt{r^2-y^2}}^{\infty} 1-\left(1+\frac{s(x^2+y^2)^{-\alpha/2}}{m}\right)^{-m}\mathrm{d}x\right]\frac{\mathrm{d}y}{(r-y_n)}\right)\right]. \quad (25)$$

Proof: See Appendix E. ∎

Lemma 15. *Conditioned on the event $\mathcal{E}_n$, serving distance R, and the distance of the n^{th} closest line from the origin Y_n, the Laplace transform of the distribution of the interference from the nodes located on the lines that are farther than the serving distance R is*

$$\mathcal{L}_{I_{out}}(s|r,y_n,\mathcal{E}_n) = \exp\left[-2\pi\lambda_l\int_{r}^{\infty} 1-\exp\left[-2\lambda_v \times \int_{0}^{\infty} 1-\left(1+\frac{s(x^2+y^2)^{-\alpha/2}}{m}\right)^{-m}\mathrm{d}x\right]\mathrm{d}y\right]. \quad (26)$$

Proof: See Appendix F. ∎

The aggregate interference at the typical receiver is given by $I = I_0 + I_{in} + I_n + I_{ann} + I_{out}$. Conditioned on $\mathcal{E}_n$, R, and Y_n, the five components of interference are mutually independent and hence, the conditional Laplace transform of the distribution of total interference power is

$$\mathcal{L}_I(s|r,y_n,\mathcal{E}_n) = \mathcal{L}_{I_0}(s|r,y_n,\mathcal{E}_n)\mathcal{L}_{I_{in}}(s|r,y_n,\mathcal{E}_n) \times \mathcal{L}_{I_n}(s|r,y_n,\mathcal{E}_n)\mathcal{L}_{I_{ann}}(s|r,y_n,\mathcal{E}_n)\mathcal{L}_{I_{out}}(s|r,y_n,\mathcal{E}_n). \quad (27)$$

In case of event $\mathcal{E}_0$, the five different sources of interference mentioned earlier is reduced to three since the typical line and the line containing the serving node are the same and there are no lines closer than the typical line. Therefore, the sources of interference in this case are: (i) the set of nodes on the typical line, (ii) the set of nodes on the lines that are closer than the serving distance R, and (iii) the set of nodes on the lines that are farther than the serving distance R. We denote the interference from the three sets of nodes by I_0, I_{in}, and I_{out}, respectively. The conditional Laplace transform of distribution of the interference from these three sources can be directly obtained from the results in Lemmas 11, 14, and 15 by substituting $\mathcal{E}_0$ and $Y_0 = 0$ in place of $\mathcal{E}_n$ and Y_n, as given in the following Corollary.

Corollary 5. *Conditioned on the event $\mathcal{E}_0$ and the serving distance R, the Laplace transform of interference power distribution is*

$$\mathcal{L}_I(s|r,\mathcal{E}_0) = \mathcal{L}_{I_0}(s|r,\mathcal{E}_0)\mathcal{L}_{I_{in}}(s|r,\mathcal{E}_0)\mathcal{L}_{I_{out}}(s|r,\mathcal{E}_0), \quad (28)$$

where

$$\mathcal{L}_{I_0}(s|r,\mathcal{E}_0) = \exp\left[-2\lambda_v\int_{r}^{\infty} 1-\left(1+\frac{sx^{-\alpha}}{m_0}\right)^{-m_0}\mathrm{d}x\right], \quad (29)$$

$$\mathcal{L}_{I_{in}}(s|r,\mathcal{E}_0) = \exp\left[\left(-2\pi\lambda_l\int_{0}^{r} e^{-2\lambda_v\sqrt{r^2-z^2}}\mathrm{d}z\right)\left(1-\int_{0}^{r}\exp\left[-2\lambda_v \times \int_{\sqrt{r^2-y^2}}^{\infty} 1-\left(1+\frac{s(x^2+y^2)^{-\alpha/2}}{m}\right)^{-m}\mathrm{d}x\right]\frac{\mathrm{d}y}{r}\right)\right], \quad (30)$$

and

$$\mathcal{L}_{I_{out}}(s|r,\mathcal{E}_0) = \exp\left[-2\pi\lambda_l\int_{r}^{\infty} 1-\exp\left[-2\lambda_v \times \int_{0}^{\infty} 1-\left(1+\frac{s(x^2+y^2)^{-\alpha/2}}{m}\right)^{-m}\mathrm{d}x\right]\mathrm{d}y\right]. \quad (31)$$

Now that we have determined the Laplace transform of distribution of interference power from all the components for both the cases $\mathcal{E}_n$ and $\mathcal{E}_0$, we will derive the coverage probability next.

F. Coverage Probability

The coverage probability is formally defined as the probability with which the SIR measured at the receiver exceeds a predetermined threshold β required for a successful communication. Using the results derived thus far, the total coverage probability at the typical receiver can be obtained in terms of the conditional Laplace transform of the distribution of the interference power as given in the following theorem.

Theorem 1. *The coverage probability of the typical receiver* $\mathtt{P_c}$ *is*

$$\mathtt{P_c} = \mathbb{P}(\mathcal{E}_0)\sum_{k=0}^{m_0-1}\int_{0}^{\infty}\frac{(-m_0\beta)^k}{r^{-k\alpha}k!}\left[\frac{\partial^k}{\partial s^k}\mathcal{L}_I(s|r,\mathcal{E}_0)\right]_{s=m_0\beta r^\alpha} f_R(r|\mathcal{E}_0)\mathrm{d}r + \sum_{n=1}^{\infty}\sum_{k=0}^{m-1}\int_{0}^{\infty}\int_{y_n}^{\infty}\frac{(-m\beta)^k}{r^{-k\alpha}k!}\left[\frac{\partial^k}{\partial s^k}\mathcal{L}_I(s|r,\mathcal{E}_n,y_n)\right]_{s=m\beta r^\alpha} \times \mathbb{P}(\mathcal{E}_n|Y_n)f_R(r|\mathcal{E}_n,y_n)f_{Y_n}(y_n)\mathrm{d}r\mathrm{d}y_n. \quad (32)$$

Proof: The coverage probability can be computed as

$$\begin{aligned}\mathtt{P_c} &= \mathbb{P}(\mathtt{SIR}>\beta) = \sum_{i=0}^{\infty}\mathbb{P}(\mathcal{E}_i)\mathbb{P}(\mathtt{SIR}>\beta|\mathcal{E}_i)\\ &= \mathbb{P}(\mathcal{E}_0)\mathbb{P}(\mathtt{SIR}>\beta|\mathcal{E}_0) + \sum_{n=1}^{\infty}\mathbb{E}_{Y_n}\Big[\mathbb{P}(\mathcal{E}_n|Y_n)\mathbb{P}(\mathtt{SIR}>\beta|\mathcal{E}_n,Y_n)\Big]\\ &= \mathbb{P}(\mathcal{E}_0)\mathbb{E}_R\Big[\mathbb{P}(\mathtt{SIR}>\beta|\mathcal{E}_0,R)\Big] + \sum_{n=1}^{\infty}\mathbb{E}_{Y_n}\Big[\mathbb{P}(\mathcal{E}_n|Y_n)\mathbb{E}_R\Big[\mathbb{P}(\mathtt{SIR}>\beta|\mathcal{E}_n,R,Y_n)\Big]\Big]\\ &= \mathbb{P}(\mathcal{E}_0)\int_{0}^{\infty}\mathbb{P}(\mathtt{SIR}>\beta|\mathcal{E}_0,R)f_R(r|\mathcal{E}_0)\mathrm{d}r + \sum_{n=1}^{\infty}\int_{0}^{\infty}\int_{y_n}^{\infty}\mathbb{P}(\mathtt{SIR}>\beta|\mathcal{E}_n,R,Y_n)\mathbb{P}(\mathcal{E}_n|Y_n) \times f_R(r|\mathcal{E}_n,y_n)f_{Y_n}(y_n)\mathrm{d}r\mathrm{d}y_n. \quad (33)\end{aligned}$$

Following the same approach presented in [29]–[31], we can obtain the final expression by rewriting the conditional coverage probability in (33) in terms of derivative of Laplace transform of the distribution of the interference power. This completes the proof. ∎

G. Asymptotic Characteristics of Coverage Probability

In this subsection, we compute the coverage probability for extremely low values of line density. As expected, the coverage probability of the typical receiver asymptotically converges to that of a 1D PPP with node density λ_v. We show this mathematically by applying the limit $\lambda_l \to 0$ on the expressions for association probability $\mathbb{P}(\mathcal{E}_0)$ and the coverage probability $\mathtt{P_c}$ in the following Lemmas.

Lemma 16. *As the density of lines tends to zero ($\lambda_l \to 0$), the typical receiver connects to its nearest node on the typical line with a probability 1.*

Proof: By applying the limit $\lambda_l \to 0$ on $\mathbb{P}(\mathcal{E}_0)$, we get

$$\begin{aligned}
&\lim_{\lambda_l \to 0} \mathbb{P}(\mathcal{E}_0) \\
&= \lim_{\lambda_l \to 0} \int_0^\infty \exp\left[-2\pi\lambda_l \int_0^{s_0} 1 - e^{-2\lambda_v \sqrt{s_0^2 - z^2}} \mathrm{d}z\right] 2\lambda_v e^{-2\lambda_v s_0} \mathrm{d}s_0 \\
&\overset{(a)}{=} \int_0^\infty \lim_{\lambda_l \to 0} \exp\left[-2\pi\lambda_l \int_0^{s_0} 1 - e^{-2\lambda_v \sqrt{s_0^2 - z^2}} \mathrm{d}z\right] 2\lambda_v e^{-2\lambda_v s_0} \mathrm{d}s_0 \\
&\overset{(b)}{=} \int_0^\infty 2\lambda_v \exp(-2\lambda_v s_0) \mathrm{d}s_0 = 1,
\end{aligned}$$

where (a) follows from the application of Dominated Convergence theorem (DCT) and (b) follows from the limit of the first term in the integrand which evaluates to 1. ∎

Lemma 17. *As the line density approaches zero ($\lambda_l \to 0$), the coverage probability of the typical receiver converges to that of a 1D PPP with node density λ_v and is given by*

$$\mathtt{P_c}^{(1)} = \sum_{k=0}^{m_0 - 1} \int_0^\infty \frac{(-m_0\beta)^k}{r^{-k\alpha} k!} \left[\frac{\partial^k}{\partial s^k} \mathcal{L}_I(s|r)\right]_{s = m_0 \beta r^\alpha} 2\lambda_v e^{-2\lambda_v r} \mathrm{d}r, \tag{34}$$

where

$$\mathcal{L}_I(s|r) = \exp\left[-2\lambda_v \int_r^\infty 1 - \left(1 + \frac{s x^{-\alpha}}{m_0}\right)^{-m_0} \mathrm{d}x\right]. \tag{35}$$

Proof: We have already shown in Lemma 16 that the typical receiver connects to its closest node on the same line with a probability 1. Therefore, the serving distance under the asymptotic condition $\lambda_l \to 0$ follows the same distribution as that of S_0 given in Corollary 1. Therefore, the asymptotic PDF of the serving distance is given by $f_R(r) = 2\lambda_v \exp(-2\lambda_v r)$. The next step is to characterize the interference experienced at the typical receiver in this case. This can simply be calculated by applying the limit $\lambda_l \to 0$ on the Laplace transform of the interference power distribution given in Corollary 5 as follows:

$$\begin{aligned}
\mathcal{L}_I(s|r) = \Big(\lim_{\lambda_l \to 0} \mathcal{L}_{I_0}(s|r, \mathcal{E}_0)\Big) \Big(\lim_{\lambda_l \to 0} \mathcal{L}_{I_{in}}(s|r, \mathcal{E}_0)\Big) \\
\times \Big(\lim_{\lambda_l \to 0} \mathcal{L}_{I_{out}}(s|r, \mathcal{E}_0)\Big)
\end{aligned}$$

$$= \exp\left[-2\lambda_v \int_r^\infty 1 - \left(1 + \frac{s x^{-\alpha}}{m_0}\right)^{-m_0} \mathrm{d}x\right].$$

Using the asymptotic serving distance distribution and Laplace transform of interference power distribution, the coverage probability can be computed by following the same approach presented in Theorem 1. ∎

As the density of lines approaches infinity ($\lambda_l \to \infty$) and the density of nodes tends to zero ($\lambda_v \to 0$) while the overall density of nodes remains the same ($\mu_l \lambda_v = \lambda_a$), the coverage probability of the typical receiver converges to that of a 2D PPP with density λ_a. While this can be proven mathematically, we skip the proof due to space limitations. A detailed account of this result will be presented in our follow-up work.

H. Area Spectral Efficiency

Area spectral efficiency is defined as the average number of bits transmitted per unit time per unit bandwidth per unit area. For the setup presented in Section III, assuming that each receiver node connects to its closest transmitting node, the number of concurrently active links in a given area is limited by the number of active transmitters in the region. Thus, the ASE can be computed as

$$\mathtt{ASE} = \lambda_a \log_2(1 + \beta)\mathtt{P_c} \quad \text{bits/s/Hz/km}^2, \tag{36}$$

where λ_a is the density of active transmitting nodes given by $\lambda_a = \mu_l \lambda_v$ and the coverage probability $\mathtt{P_c}$ is given by (32) in Theorem 1. The impact of the line and node densities on the $\mathtt{ASE}$ is discussed in the next section.

V. Numerical Results and Discussion

In this section, we verify the accuracy of our analytical results by comparing the coverage probabilities evaluated using the theoretical expressions with the results obtained from the Monte-Carlo simulations. We also analyze the trends in coverage probability as a function of network parameters. We then demonstrate that the coverage probability for the setup asymptotically converges to that of 1D and 2D PPPs for extreme values of line and node densities. We also provide some design insights into the deployment of RSUs by analyzing the trends in ASE.

A. Coverage Probability

We simulate the Cox process model described in Section III in MATLAB with line density $\mu_l = 35$ km/km^2, node density $\lambda_v = 35$ nodes/km, and path-loss exponent $\alpha = 4$. We observe that our analytical results match exactly with the empirical coverage probability evaluated using Monte-Carlo simulations as depicted in Fig. 5. The key network parameters that have an impact on the coverage probability are line density, node density, severity of fading and path-loss exponent. We will next study the impact of each of these parameters separately on the coverage probability.

Impact of line density. We compute the coverage probability of the typical receiver for node density of $\lambda_v = 35$ nodes/km and different line densities of $\mu_l = 15, 25, 35$, and 45 km/km^2. It can be observed from Fig. 6 that the coverage probability

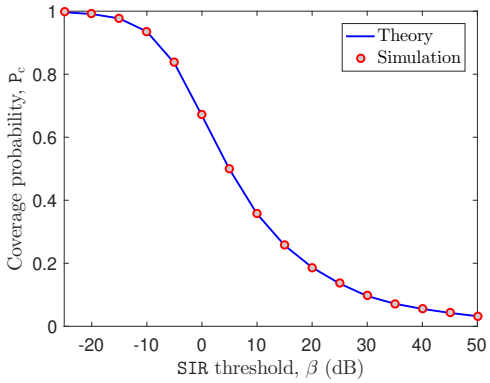

Fig. 5. Coverage probability of the typical receiver as a function of SIR threshold ($\mu_l = 35$ km/km^2, $\lambda_v = 35$ nodes/km, $m_0 = m = 1$, and $\alpha = 4$).

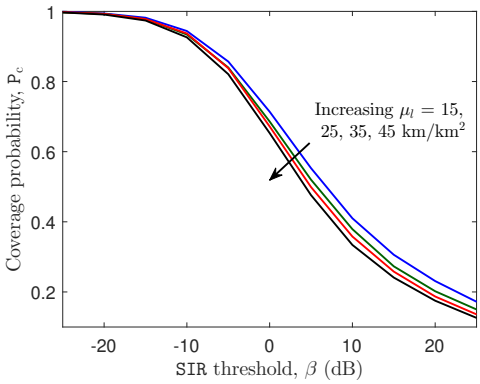

Fig. 6. Coverage probability of the typical receiver as a function of SIR threshold ($\lambda_v = 35$ nodes/km, $m_0 = m = 1$, and $\alpha = 4$).

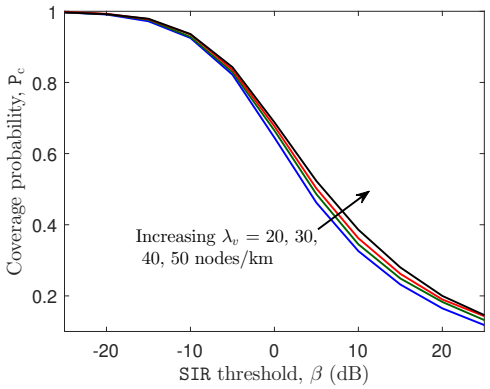

Fig. 7. Coverage probability of the typical receiver as a function of SIR threshold ($\mu_l = 35$ km/km^2, $m_0 = m = 1$, and $\alpha = 4$).

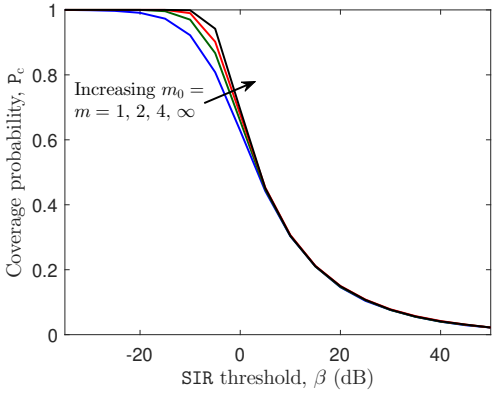

Fig. 8. Coverage probability of the typical receiver as a function of SIR threshold ($\mu_l = 35$ km/km^2, $\lambda_v = 35$ nodes/km, and $\alpha = 4$).

decreases as the line density increases. This trend in the coverage probability can be easily understood by examining the case where the receiver connects to a node on the typical line. In this case, an increase in the line density does not have any effect on the serving distance, however, it increases the interference power due to the reduced distance between the typical receiver and interfering nodes on other lines.

Impact of node density. We compare the coverage probability of the typical receiver for node densities of $\lambda_v = 20, 30, 40$, and 50 nodes/km as a function of SIR threshold β. It can be observed from Fig. 7 that the coverage probability increases as the density of nodes on the lines increases. Recall that the distance from the typical receiver at the origin to any node on a line involves two components: (i) perpendicular distance of the line from the origin, and (ii) the distance of the node (along the line) from the projection of the origin onto the line. When the density of nodes increases, the nodes come closer along the direction of the line, which decreases the second component of distance described above. Consequently, the decrement in the distance from the typical receiver to the nodes located on the lines that are closer to the origin is relatively more than the decrement in the distance to the nodes located on the lines that are farther away from the origin. This increases the desired signal power at a faster rate than the interference power, thus improving the SIR and hence the coverage probability at the typical receiver.

Impact of fading. We study the impact of fading on coverage in Fig. 8, where the coverage probability of the typical receiver is computed for fading parameters $m_0 = m = 1$, 2, 4, and ∞. From Fig. 8, it can be observed that the variance of SIR decreases in the operational regime of interest as m_0 and m increase and this trend in coverage probability is consistent with those of well-investigated 1D and 2D PPPs.

Impact of path-loss exponent. We plot the coverage probability of the typical receiver as a function of SIR threshold β for path-loss exponent values of $\alpha = 2.5$, 3, 3.5, and 4 as shown in Fig. 9. While decreasing the value of path-loss exponent increases the desired signal power, it also increases the interference power at the typical receiver at a faster rate, thereby decreasing the overall SIR and hence the coverage probability.

Asymptotic Characteristics of Coverage Probability. We plot the coverage probability of the typical receiver for some extreme values of line and node densities as shown in Fig. 10. It can be observed that the coverage probability for moderate values of line and node density ($\mu_l = 35$ km/km^2, $\lambda_v = 35$ nodes/km) differs significantly from that of 1D and 2D PPP models which are often used to model vehicular networks. However, for a relatively low line density ($\mu_l = 10$ km/km^2), the coverage probability for this setup converges to that of a 1D PPP, thereby verifying the asymptotic results derived

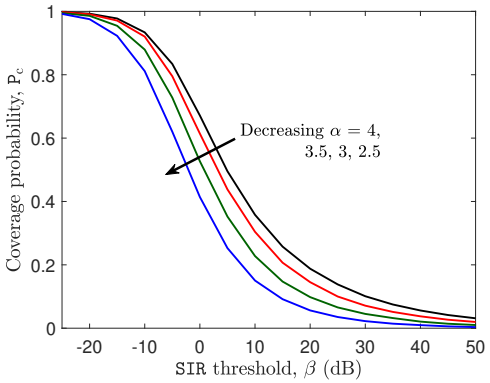

Fig. 9. Coverage probability of the typical receiver as a function of SIR threshold ($\mu_l = 35$ km/km^2, $\lambda_v = 35$ nodes/km, and $m_0 = m = 1$).

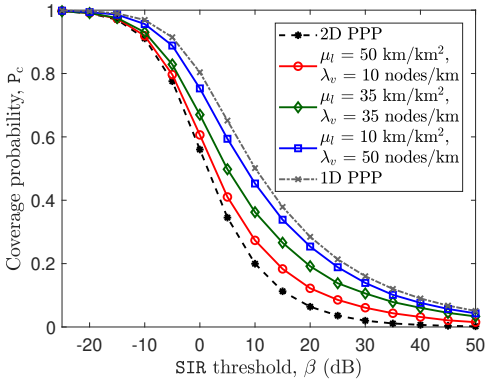

Fig. 10. Coverage probability of the typical receiver as a function of SIR threshold ($m_0 = m = 1$ and $\alpha = 4$).

in Lemma 17. Similarly, for a high line density and low node density ($\mu_l = 50$ km/km^2, $\lambda_v = 10$ nodes/km), we can observe that the coverage probability for this setup converges to that of a homogeneous 2D PPP with equivalent node density of $\lambda_a = \mu_l \lambda_v = 500$ nodes/km^2 as stated in Section IV-G.

B. Area Spectral Efficiency

In this subsection, we analyze the impact of line and node densities on the ASE of the network. As the node density increases, both the coverage probability and the number of concurrently active links in a given region increase, thereby improving the ASE. On the other hand, with an increase in line density, the coverage probability of the typical receiver degrades while the number of active links in the network increases. In order to understand the combined effect, we compute the ASE of the network as a function of node density for different values of line densities as shown in Fig. 11. Since the nodes considered in our setup jointly represent the vehicular nodes and RSUs, one can modify the density of nodes in a given area by deploying the RSUs in the network. From Fig. 11, it can be observed that the minimum density of nodes required to achieve a certain ASE increases as the density of lines decreases. Therefore, the areas with sparse distribution of roads require a denser deployment of RSUs as compared to the areas with dense roads in order to achieve the same ASE.

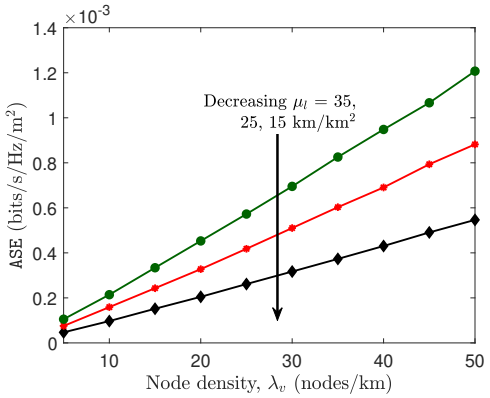

Fig. 11. ASE of the network as a function of node density λ_v ($m_0 = m = 1$ and $\alpha = 4$).

VI. Conclusion

In this paper, we have presented an analytical method for the coverage analysis of a vehicular network in which the locations of nodes are confined to road systems. We have modeled the roads by a PLP and the nodes on each road by a homogeneous 1D PPP. Assuming that the typical receiver connects to its closest node in the network, we began our analysis with the derivation of several distance distributions which were necessary to determine the desired signal power at the typical receiver. We then computed the conditional distribution of lines in order to characterize the interference at the typical receiver. We then derived an exact expression for SIR-based coverage probability of the typical receiver in terms of the derivative of Laplace transform of interference power distribution. We also studied the asymptotic characteristics of the coverage probability for our setup. We have verified the accuracy of our analytical results numerically by comparing them with the results obtained from Monte-Carlo simulations. We also computed the ASE of the network as a function of line and node densities and provided some insights into the deployment of RSUs to achieve the desired performance.

This work has numerous extensions. First and foremost, the proposed model as well as the canonical analysis presented in this paper can be readily applied to study other metrics of interest, such as information throughput and latency, which were not directly analyzed in this paper. Another meaningful extension of the current work could be to analyze the performance of the network for an enhanced system model which includes realistic blockage models and sophisticated channel access schemes such as CSMA. The proposed approach can also be easily specialized to study the vehicular network performance under specific system constraints, such as those imposed by the mmWave frequencies, thus making the analysis relevant to a particular technology such as 5G. From stochastic geometry perspective, it will be useful to develop appropriate generative models for the proposed setup that simplify the analysis without compromising the accuracy of the results. Finally, while the proposed model is a reasonable canonical model for vehicular networks, there is always scope for making such models more accurate (often at the cost of reduced tractability) by obtaining network parameters from

the actual data [32]. Therefore, another worthwhile extension of this work is to take a data-driven approach to vehicular network modeling, which will provide useful insights into the parameter ranges that are of interest in different morphologies.

APPENDIX

A. Proof of Lemma 4

The CDF of U_n conditioned on Y_n is

$$\begin{aligned} F_{U_n}(u_n|y_n) &= 1-\mathbb{P}(U_n > u_n|Y_n) \\ &= 1-\mathbb{P}\Big(N_v\big(b(o,u_n)\big)=0|Y_n\Big), \end{aligned}$$

where $N_v(b(o,u_n))$ denotes the number of nodes within the disc of radius u_n centered at o. Therefore, we need to find the probability that there are no nodes on any of the lines that are closer than Y_n that intersect the disc $b(o,u_n)$. We know that there are $n-1$ lines whose distance from the origin is uniformly distributed in the range $(0,y_n)$. Depending on the range of u_n, there are two possible cases: (i) if u_n is smaller than y_n, then the number of lines intersecting the disc $b(o,u_n)$ follows a binomial distribution with parameters $n-1$ and $\frac{u_n}{y_n}$, and (ii) if u_n exceeds y_n, then all the $n-1$ lines intersect the disc $b(o,u_n)$. Thus, we obtain a piece-wise conditional CDF for U_n as follows:

$$\begin{aligned} &F_{U_n}(u_n|y_n) \\ &= \begin{cases} 1-\sum_{j=0}^{n-1}\mathbb{P}\Big(N_v\big(b(o,u_n)\big)=0|N_l\big(b(o,u_n)\big)=j,Y_n\Big) \\ \qquad\times\mathbb{P}\Big(N_l\big(b(o,u_n)\big)=j|Y_n\Big), & 0\le u_n<y_n, \\ 1-\prod_{i=1}^{n-1}\mathbb{P}\Big(N_v\big(L_i\cap b(o,u_n)\big)=0|Y_n\Big), & y_n\le u_n<\infty \end{cases} \\ &\overset{(a)}{=} \begin{cases} 1-\sum_{j=0}^{n-1}\Big(\mathbb{P}\Big(N_v\big(L\cap b(o,u_n)\big)=0|Y_n\Big)\Big)^j \\ \qquad\times\mathbb{P}\Big(N_l\big(b(o,u_n)\big)=j|Y_n\Big), & 0\le u_n<y_n, \\ 1-\Big[\mathbb{P}\Big(N_v\big(L\cap b(o,u_n)\big)=0|Y_n\Big)\Big]^{n-1} & y_n\le u_n<\infty, \end{cases} \end{aligned} \tag{37}$$

where (a) follows from the independent and identically distributed (i.i.d.) locations of the nodes on the lines. In step (a), L denotes an arbitrarily chosen line that intersects the disc $b(o,u_n)$. We will now derive the expression for each term in (37). For the case $0\le u_n<y_n$, we know that the number of lines intersecting the disc $b(o,u_n)$ follows a binomial distribution. Therefore,

$$\mathbb{P}\Big(N_l\big(b(o,u_n)\big)=j|Y_n\Big)=\binom{n-1}{j}\Big(\frac{u_n}{y_n}\Big)^j\Big(1-\frac{u_n}{y_n}\Big)^{n-1-j}. \tag{38}$$

We will now evaluate the probability that there are no nodes on the segment of an arbitrarily chosen line L that intersects the disc $b(o,u_n)$. We denote the perpendicular distance of the line from the origin by Z which is uniformly distributed in the range $(0,u_n)$ for the first case. Conditioned on Z, the probability that there are no nodes on the segment that intersects $b(o,u_n)$ is given by $\mathbb{P}\Big(N_v\big(L\cap b(o,u_n)\big)=0|Z,Y_n\Big)=\exp\big(-\lambda_v 2\sqrt{u_n^2-z^2}\big)$. This result follows from the void probability of 1D-PPP. By taking the expectation over Z, we obtain the probability that there are no nodes on the segment of a randomly chosen line that intersects the disc $b(o,u_n)$ as

$$\mathbb{P}\Big(N_v\big(L\cap b(o,u_n)\big)=0|Y_n\Big)=\int_0^{u_n}e^{-2\lambda_v\sqrt{u_n^2-z^2}}\frac{\mathrm{d}z}{u_n}. \tag{39}$$

Similarly, for the second case where $y_n\le u_n<\infty$, the distances of the lines that intersect the disc $b(0,u_n)$ are uniformly distributed in the range $(0,y_n)$. Therefore, the desired probability in this case is given by

$$\mathbb{P}\Big(N_v\big(L\cap b(o,u_n)\big)=0|Y_n\Big)=\int_0^{y_n}e^{-2\lambda_v\sqrt{u_n^2-z^2}}\frac{\mathrm{d}z}{y_n}. \tag{40}$$

Upon substituting (38), (39), and (40) in (37) and simplifying the resulting expression, we obtain the final result. The PDF of U_n can then be computed by taking the derivative of $F_{U_n}(u_n|y_n)$ with respect to u_n.

B. Proof of Lemma 5

The CDF of V_n conditioned on Y_n is

$$\begin{aligned} F_{V_n}(v_n|y_n) &= 1-\mathbb{P}(V_n>v_n|Y_n) \\ &= 1-\mathbb{P}\Big(N_v\big(b(o,v_n)\setminus b(o,y_n)\big)=0|Y_n\Big) \\ &\overset{(a)}{=} 1-\sum_{n_l=0}^{\infty}\mathbb{P}\Big(N_l\big(b(o,v_n)\setminus b(o,y_n)\big)=n_l|Y_n\Big) \\ &\quad\times\Big(\mathbb{P}\Big(N_v\big(L\cap\{b(o,v_n)\setminus b(o,y_n)\}\big)=0|Y_n\Big)\Big)^{n_l}, \end{aligned} \tag{41}$$

where (a) follows from the i.i.d. locations of nodes on the lines. Note that L denotes an arbitrarily chosen line whose distance from the origin is greater than v_n and smaller than y_n. From the definition of PLP, we know that the number of lines whose distances from the origin are in the range (y_n,v_n) follows a Poisson distribution with mean $2\pi\lambda_l(v_n-y_n)$. Thus,

$$\mathbb{P}\Big(N_l\big(b(o,v_n)\setminus b(o,y_n)\big)=n_l|Y_n\Big)=\frac{\exp\big(-2\pi\lambda_l(v_n-y_n)\big)\big(2\pi\lambda_l(v_n-y_n)\big)^{n_l}}{n_l!}. \tag{42}$$

The evaluation of the second term in the equation (41) is similar to that of (39) in the proof of Lemma 4. The only change is that the distances of the lines in this case are uniformly distributed in the range (y_n,v_n). Hence, the desired probability is obtained as

$$\mathbb{P}\Big(N_v\big(L\cap\{b(o,v_n)\setminus b(o,y_n)\}\big)=0|Y_n\Big)=\int_{y_n}^{v_n}\exp\big(-2\lambda_v\sqrt{v_n^2-z^2}\big)\frac{1}{(v_n-y_n)}\mathrm{d}z. \tag{43}$$

Substituting (42) and (43) in (41), we obtain the final expression. The conditional PDF of V_n can then be obtained by taking the derivative of $F_{V_n}(v_n|y_n)$ w.r.t. v_n.

C. Proof of Lemma 10

The conditional PMF of number of lines can be computed as

$$\mathbb{P}\Big(N_l\big(b(o,r)\setminus b(o,y_n)\big)=k\big|\mathcal{E}_n,Y_n,R\Big) \overset{(a)}{=} \frac{\mathbb{P}\Big(\mathcal{E}_n\big|N_l\big(b(o,r)\setminus b(o,y_n)\big)=k,Y_n,R\Big)}{\mathbb{P}\Big(\mathcal{E}_n|Y_n,R\Big)} \times \mathbb{P}\Big(N_l\big(b(o,r)\setminus b(o,y_n)\big)=k|Y_n,R\Big), \quad (44)$$

where (a) follows from the application of Bayes' theorem. We now need to determine each term in (44) to compute the desired conditional PMF. The first term in the numerator is nothing but the probability that there are no nodes inside a disc of radius r centered at the origin, given that there are k lines that are farther than y_n and closer than r. In addition to these k lines, there are $n-1$ lines that are closer than y_n, one line at a distance of y_n, and the typical line that intersect the disc $b(o,r)$. Therefore, the probability that there are no nodes on any of these lines that intersect the disc $b(o,r)$ can be computed as follows:

$$\begin{aligned}
&\mathbb{P}\Big(\mathcal{E}_n\big|N_l\big(b(o,r)\setminus b(o,y_n)\big)=k,Y_n,R\Big)\\
&=\mathbb{P}\Big(N_v\big(b(o,r)\big)=0\big|N_l\big(b(o,r)\setminus b(o,y_n)\big)=k,Y_n,R\Big)\\
&=\mathbb{P}\left[N_v\big(L_0\cap b(o,r)\big)=0|Y_n,R\right]\\
&\quad\times\left[\prod_{i=1}^{n-1}\mathbb{P}\Big(N_v\big(L_i\cap b(o,r)\big)=0|Y_n,R\Big)\right]\\
&\quad\times\mathbb{P}\left(N_v\big(L_n\cap b(o,r)\big)=0|Y_n,R\right)\\
&\quad\times\left[\prod_{j=1}^{k}\mathbb{P}\Big(N_v\big(L_{n+j}\cap b(o,r)\big)=0|Y_n,R\Big)\right] \quad (45)\\
&=e^{-2\lambda_v r}\left[\int_0^{y_n}e^{-2\lambda_v\sqrt{r^2-y^2}}\frac{\mathrm{d}y}{y_n}\right]^{n-1}e^{-2\lambda_v\sqrt{r^2-y_n^2}}\\
&\quad\times\left[\int_{y_n}^{r}e^{-2\lambda_v\sqrt{r^2-y^2}}\frac{\mathrm{d}y}{(r-y_n)}\right]^{k}. \quad (46)
\end{aligned}$$

The second term in the numerator in (44) is the probability that there are k lines that are farther than y_n and closer than r. Since both r and y_n are fixed, the number of lines that are farther than y_n and closer than r simply follows a Poisson distribution with mean $2\pi\lambda_l(r-y_n)$. Therefore, the second term in the numerator is given by

$$\mathbb{P}\Big(N_l\big(b(o,r)\setminus b(o,y_n)\big)=k|Y_n,R\Big)= \frac{\exp\big(-2\pi\lambda_l(r-y_n)\big)\big(2\pi\lambda_l(r-y_n)\big)^k}{k!}. \quad (47)$$

The denominator in (44) is the probability of occurrence of event $\mathcal{E}_n$ conditioned on both Y_n and R. This is nothing but the probability that there are no nodes inside the disc of radius r. This can be easily computed using law of total probability as follows:

$$\begin{aligned}
&\mathbb{P}\Big(\mathcal{E}_n|Y_n,R\Big)\\
&=\sum_{k=0}^{\infty}\mathbb{P}\Big(\mathcal{E}_n\big|N_l\big(b(o,r)\setminus b(o,y_n)\big)=k,Y_n,R\Big)\\
&\quad\times\mathbb{P}\Big(N_l\big(b(o,r)\setminus b(o,y_n)\big)=k|Y_n,R\Big) \quad (48)\\
&\overset{(a)}{=}e^{-2\lambda_v r}\left[\int_0^{y_n}e^{-2\lambda_v\sqrt{r^2-y^2}}\frac{\mathrm{d}y}{y_n}\right]^{n-1}e^{-2\lambda_v\sqrt{r^2-y_n^2}}e^{-2\pi\lambda_l(r-y_n)}\\
&\quad\times\sum_{k=0}^{\infty}\frac{\big(2\pi\lambda_l(r-y_n)\big)^k}{k!}\left[\int_{y_n}^{r}\frac{e^{-2\lambda_v\sqrt{r^2-y^2}}}{(r-y_n)}\mathrm{d}y\right]^k\\
&=\exp\left[-2\lambda_v r-2\lambda_v\sqrt{r^2-y_n^2}-2\pi\lambda_l\int_{y_n}^{r}1-e^{(-2\lambda_v\sqrt{r^2-y^2})}\mathrm{d}y\right]\\
&\quad\times\left[\int_0^{y_n}e^{(-2\lambda_v\sqrt{r^2-y^2})}\frac{\mathrm{d}y}{y_n}\right]^{n-1}, \quad (49)
\end{aligned}$$

where (a) follows from substituting (46) and (47) in (48).

Substituting (46), (47), and (49) in (44), we obtain the final expression.

D. Proof of Lemma 13

We know that there are $n-1$ lines (excluding the typical line) closer than Y_n whose distances from the origin are uniformly distributed in the range $(0,y_n)$. The Laplace transform of distribution of interference from an arbitrarily chosen line L, conditioned on its distance from the origin Y is given by

$$\mathcal{L}_{I_L}(s|r,y_n,\mathcal{E}_n,y) =\exp\left[-2\lambda_v\int_{\sqrt{r^2-y^2}}^{\infty}1-\Big(1+\frac{s(x^2+y^2)^{-\alpha/2}}{m}\Big)^{-m}\mathrm{d}x\right]. \quad (50)$$

This expression is similar to the result obtained in Lemma 12. The lower limit of the integral follows from the condition that there must be no nodes closer than r. Now, taking the expectation over Y which is uniformly distributed in the range $(0,y_n)$, we obtain the conditional Laplace transform of distribution of interference from a single line as

$$\begin{aligned}
\mathcal{L}_{I_L}(s|r,y_n,\mathcal{E}_n)&=\int_0^{y_n}\mathcal{L}_{I_L}(s|r,y_n,\mathcal{E}_n,y)\frac{\mathrm{d}y}{y_n}\\
&=\int_0^{y_n}\exp\left[-2\lambda_v\int_{\sqrt{r^2-y^2}}^{\infty}1-\Big(1+\frac{s(x^2+y^2)^{-\alpha/2}}{m}\Big)^{-m}\mathrm{d}x\right]\frac{\mathrm{d}y}{y_n}. \quad (51)
\end{aligned}$$

Owing to the i.i.d. locations of nodes on the lines, the conditional Laplace transform of distribution of interference from the nodes on all the $n-1$ lines is given by

$$\mathcal{L}_{I_{in}}(s|r,y_n,\mathcal{E}_n)=\big(\mathcal{L}_{I_L}(s|r,y_n,\mathcal{E}_n)\big)^{n-1}=\left(\int_0^{y_n}\exp\left[-2\lambda_v\times\int_{\sqrt{r^2-y^2}}^{\infty}1-\Big(1+\frac{s(x^2+y^2)^{-\alpha/2}}{m}\Big)^{-m}\mathrm{d}x\right]\frac{\mathrm{d}y}{y_n}\right)^{n-1}. \quad (52)$$

E. Proof of Lemma 14

We know that the distances of the random number of lines that are farther than y_n and closer than r are uniformly distributed in the range (y_n, r). As given in (50), the Laplace transform of interference from an arbitrarily chosen line L conditioned on the distance of the line from the origin Y is

$$\mathcal{L}_{I_L}(s|r, y_n, \mathcal{E}_n, y) = \exp\left[-2\lambda_v \int_{\sqrt{r^2-y^2}}^{\infty} 1 - \Big(1 + \frac{s(x^2+y^2)^{-\alpha/2}}{m}\Big)^{-m} \mathrm{d}x\right].$$

Thus, the conditional Laplace transform of distribution of interference from a single line is

$$\mathcal{L}_{I_L}(s|r, y_n, \mathcal{E}_n) = \int_{y_n}^{r} \exp\left[-2\lambda_v \int_{\sqrt{r^2-y^2}}^{\infty} 1 - \Big(1 + \frac{s(x^2+y^2)^{-\alpha/2}}{m}\Big)^{-m} \mathrm{d}x\right] \frac{\mathrm{d}y}{(r-y_n)}. \tag{53}$$

Owing to the i.i.d. locations of nodes on the lines, the conditional Laplace transform of interference distribution from all the lines that are farther than Y_n and closer than R is

$$\mathcal{L}_{I_{ann}}(s|r, y_n, \mathcal{E}_n) = \sum_{i=0}^{\infty} \mathbb{P}\Big(N_l\big(b(o,r) \setminus b(o,y_n)\big) = i\Big)\Big(\mathcal{L}_{I_L}(s|r, y_n, \mathcal{E}_n)\Big)^i \tag{54}$$

$$\stackrel{(a)}{=} \exp\left[\left(-2\pi\lambda_l \int_{y_n}^{r} e^{-2\lambda_v\sqrt{r^2-z^2}} \mathrm{d}z\right)\Big(1 - \mathcal{L}_{I_L}(s|r, y_n, \mathcal{E}_n)\Big)\right], \tag{55}$$

where (a) follows from the substitution of the PMF given by Lemma 10 in (54). Substituting (53) in (55), we obtain the final expression.

F. Proof of Lemma 15

Following the same approach as in Lemma 14, we determine the conditional Laplace transform of distribution of interference from an arbitrary line L at a distance Y from the origin as follows:

$$\mathcal{L}_{I_L}(s|r, y_n, \mathcal{E}_n, y) = \exp\left[-2\lambda_v \int_{0}^{\infty} 1 - \Big(1 + \frac{s(x^2+y^2)^{-\alpha/2}}{m}\Big)^{-m} \mathrm{d}x\right]. \tag{56}$$

Owing to the independent distribution of nodes on the lines, for a given realization of the line process, the conditional Laplace transform of interference distribution is simply the product of the Laplace transform of distribution of interference from each of these lines. Therefore, we can write the Laplace transform of distribution of interference conditioned on the line process $\Phi_{l_0} \equiv \Phi_l \cup L_0$ as

$$\mathcal{L}_{I_{out}}(s|r, y_n, \mathcal{E}_n, \Phi_{l_0}) = \prod_{y \in \Psi_{l_0}} \mathcal{L}_{I_L}(s|r, y_n, \mathcal{E}_n, y), \tag{57}$$

where Ψ_{l_0} represents the set of distances of the lines from the origin, which is a 1D PPP with density $2\pi\lambda_l$ as shown in the proof of Lemma 1. By taking the expectation over Ψ_{l_0} and applying the PGFL of PPP, we obtain the desired result as follows:

$$\mathcal{L}_{I_{out}}(s|r, y_n, \mathcal{E}_n) = \exp\left[-2\pi\lambda_l \int_{r}^{\infty} 1 - \mathcal{L}_{I_L}(s|r, y_n, \mathcal{E}_n, y)\mathrm{d}y\right]. \tag{58}$$

We obtain the final expression upon substituting (56) in (58).

REFERENCES

[1] V. V. Chetlur, S. Guha, and H. S. Dhillon, "Characterization of V2V coverage in a network of roads modeled as Poisson line process," in *Proc., IEEE ICC*, May 2018.

[2] H. Hartenstein and L. P. Laberteaux, "A tutorial survey on vehicular ad hoc networks," *IEEE Commun. Magazine*, vol. 46, no. 6, pp. 164–171, Jun. 2008.

[3] S. Biswas, R. Tatchikou, and F. Dion, "Vehicle-to-vehicle wireless communication protocols for enhancing highway traffic safety," *IEEE Commun. Magazine*, vol. 44, no. 1, pp. 74–82, Jan. 2006.

[4] P. Papadimitratos, A. D. L. Fortelle, K. Evenssen, R. Brignolo, and S. Cosenza, "Vehicular communication systems: Enabling technologies, applications, and future outlook on intelligent transportation," *IEEE Commun. Magazine*, vol. 47, no. 11, pp. 84–95, Nov. 2009.

[5] H. S. Dhillon, R. K. Ganti, F. Baccelli, and J. G. Andrews, "Modeling and analysis of K-tier downlink heterogeneous cellular networks," *IEEE J. on Sel. Areas in Commun*, vol. 30, no. 3, pp. 550–560, Apr. 2012.

[6] J. G. Andrews, F. Baccelli, and R. K. Ganti, "A tractable approach to coverage and rate in cellular networks," *IEEE Trans. on Commun.*, vol. 59, no. 11, pp. 3122–3134, Nov. 2011.

[7] J. G. Andrews, A. K. Gupta, and H. S. Dhillon, "A primer on cellular network analysis using stochastic geometry," *arXiv preprint*, Oct. 2016, available online: arxiv.org/abs/1604.03183.

[8] H. ElSawy, A. Sultan-Salem, M. S. Alouini, and M. Z. Win, "Modeling and analysis of cellular networks using stochastic geometry: A tutorial," *IEEE Communications Surveys Tutorials*, vol. 19, no. 1, pp. 167–203, Firstquarter 2017.

[9] Y. Wang, K. Venugopal, A. F. Molisch, and R. W. Heath Jr., "MmWave vehicle-to-infrastructure communication: Analysis of urban microcellular networks," 2017, available online: arxiv.org/abs/1702.08122.

[10] F. Baccelli, M. Klein, M. Lebourges, and S. Zuyev, "Stochastic geometry and architecture of communication networks," *Telecommunication Systems*, vol. 7, no. 1, pp. 209–227, Jun. 1997.

[11] C. Gloaguen, F. Fleischer, H. Schmidt, and V. Schmidt, "Analysis of shortest paths and subscriber line lengths in telecommunication access networks," *Networks and Spatial Economics*, vol. 10, no. 1, pp. 15–47, Mar. 2010.

[12] F. Voss, C. Gloaguen, F. Fleischer, and V. Schmidt, "Distributional properties of Euclidean distances in wireless networks involving road systems," *IEEE J. on Sel. Areas in Commun.*, vol. 27, no. 7, pp. 1047–1055, Sep. 2009.

[13] F. Morlot, "A population model based on a Poisson line tessellation," in *Proc., Modeling and Optimization in Mobile, Ad Hoc and Wireless Networks*, May 2012, pp. 337–342.

[14] S. N. Chiu, D. Stoyan, W. S. Kendall, and J. Mecke, *Stochastic geometry and its applications*. John Wiley & Sons, 2013.

[15] M. Haenggi, *Stochastic Geometry for Wireless Networks*. Cambridge University Press, 2013.

[16] B. Blaszczyszyn, P. Muhlethaler, and Y. Toor, "Maximizing throughput of linear vehicular Ad-hoc NETworks (VANETs) – a stochastic approach," in *European Wireless Conf.*, May 2009, pp. 32–36.

[17] S. Busanelli, G. Ferrari, and R. Gruppini, "Performance analysis of broadcast protocols in VANETs with Poisson vehicle distribution," in *Intl. Conf. on ITS Telecommunications*, Aug 2011, pp. 133–138.

[18] M. J. Farooq, H. ElSawy, and M. S. Alouini, "A stochastic geometry model for multi-hop highway vehicular communication," *IEEE Trans. on Wireless Commun.*, vol. 15, no. 3, pp. 2276–2291, Mar. 2016.

[19] M. Mabiala, A. Busson, and V. Veque, "Inside VANET: Hybrid network dimensioning and routing protocol comparison," in *Proc., IEEE Veh. Technology Conf.*, Apr. 2007, pp. 227–232.

[20] M. Ni, M. Hu, Z. Wang, and Z. Zhong, "Packet reception probability of VANETs in urban intersecton scenario," in *Intl. Conf. on Connected Vehicles and Expo*, Oct. 2015, pp. 124–125.

[21] E. Steinmetz, M. Wildemeersch, T. Q. S. Quek, and H. Wymeersch, "A stochastic geometry model for vehicular communication near intersections," in *Proc., IEEE Globecom Workshops*, Dec. 2015, pp. 1–6.
[22] C. Gloaguen, F. Fleischer, H. Schmidt, and V. Schmidt, "Simulation of typical Cox Voronoi cells with a special regard to implementation tests," *Mathematical Methods of Operations Research*, vol. 62, no. 3, pp. 357–373, 2005.
[23] B. Blaszczyszyn and P. Muhlethaler, "Random linear multihop relaying in a general field of interferers using spatial Aloha," *IEEE Trans. on Wireless Commun.*, vol. 14, no. 7, pp. 3700–3714, Jul. 2015.
[24] S. Aditya, H. S. Dhillon, A. F. Molisch, and H. Behairy, "Asymptotic blind-spot analysis of localization networks under correlated blocking using a Poisson line process," *IEEE Wireless Commun. Letters*, to appear.
[25] R. Schneider and W. Weil, *Stochastic and Integral Geometry*. Springer Berlin Heidelberg, 2008.
[26] T. V. Nguyen, F. Baccelli, K. Zhu, S. Subramanian, and X. Wu, "A performance analysis of CSMA based broadcast protocol in VANETs," in *Proc., IEEE INFOCOM*, Apr. 2013.
[27] S. Subramanian, M. Werner, S. Liu, J. Jose, R. Lupoaie, and X. Wu, "Congestion control for vehicular safety: Synchronous and asynchronous MAC algorithms," in *Proc., ACM VANET*, Jun. 2012.
[28] A. Leon-Garcia, *Probability, Statistics, and Random Processes For Electrical Engineering*. Pearson Education, 2011.
[29] V. V. Chetlur and H. S. Dhillon, "Downlink coverage analysis for a finite 3D wireless network of unmanned aerial vehicles," *IEEE Trans. on Commun.*, to appear.
[30] R. Tanbourgi, H. S. Dhillon, J. G. Andrews, and F. K. Jondral, "Dual-branch MRC receivers under spatial interference correlation and Nakagami fading," *IEEE Trans. on Commun.*, vol. 62, no. 6, pp. 1830–1844, Jun. 2014.
[31] Y. J. Chun, S. L. Cotton, H. S. Dhillon, A. Ghrayeb, and M. O. Hasna, "A stochastic geometric analysis of device-to-device communications operating over generalized fading channels," *IEEE Trans. on Wireless Commun.*, vol. 16, no. 7, pp. 4151–4165, Jul. 2017.
[32] C. Gloaguen, F. Fleischer, H. Schmidt, and V. Schmidt, "Fitting of stochastic telecommunication network models via distance measures and Monte–Carlo tests," *Telecommunication Systems*, vol. 31, no. 4, pp. 353–377, Apr. 2006.

Vishnu Vardhan Chetlur received the B. E. (Hons.) degree in Electronics and Communications Engineering from the Birla Institute of Technology and Science (BITS) Pilani, India, in 2013. After his graduation, he worked as a design engineer at Redpine Signals Inc. for two years. He is currently a Ph.D. student at Virginia Tech, where his research interests include wireless communication, smart cities, and stochastic geometry. He graduated top of his class in the department of Electrical Engineering at BITS and was awarded the institute Silver medal for being ranked second in the whole institute. He was also a recipient of the BITS merit scholarship for his excellence in academics.

Harpreet S. Dhillon (S'11–M'13) received the B.Tech. degree in Electronics and Communication Engineering from IIT Guwahati, India, in 2008; the M.S. degree in Electrical Engineering from Virginia Tech, Blacksburg, VA, USA, in 2010; and the Ph.D. degree in Electrical Engineering from the University of Texas at Austin, TX, USA, in 2013. In academic year 2013-14, he was a Viterbi Postdoctoral Fellow at the University of Southern California, Los Angeles, CA, USA. He joined Virginia Tech in August 2014, where he is currently an Assistant Professor and Steven O. Lane Junior Faculty Fellow of Electrical and Computer Engineering. He has held short-term visiting positions at Bell Labs, Samsung Research America, Qualcomm Inc., and Politecnico di Torino. His research interests include communication theory, stochastic geometry, geolocation, and wireless *ad hoc* and heterogeneous cellular networks.

Dr. Dhillon is a Clarivate Analytics Highly Cited Researcher and has coauthored five best paper award recipients including the 2016 IEEE Communications Society (ComSoc) Heinrich Hertz Award, the 2015 IEEE ComSoc Young Author Best Paper Award, the 2014 IEEE ComSoc Leonard G. Abraham Prize, and two conference best paper awards at IEEE ICC 2013 and European Wireless 2014. He was named the 2018 College of Engineering Faculty Fellow and the 2017 Outstanding New Assistant Professor by Virginia Tech. His other academic honors include the 2013 UT Austin Wireless Networking and Communications Group (WNCG) leadership award, the UT Austin Microelectronics and Computer Development (MCD) Fellowship, and the 2008 Agilent Engineering and Technology Award. He currently serves as an Editor for the IEEE TRANSACTIONS ON WIRELESS COMMUNICATIONS, the IEEE TRANSACTIONS ON GREEN COMMUNICATIONS AND NETWORKING, and the IEEE WIRELESS COMMUNICATIONS LETTERS.